Utah State University

DigitalCommons@USU

5-2014

Considerations for Hood Placement and Design Downstream from a Fixed-Cone Valve

Barry Jacob Prettyman
Utah State University

Follow this and additional works at: https://digitalcommons.usu.edu/etd

Part of the Civil Engineering Commons

Utah State University
MERRILL-CAZIER LIBRARY

CONSIDERATIONS FOR HOOD PLACEMENT AND DESIGN DOWNSTREAM

FROM A FIXED-CONE VALVE

by

Barry Jacob Prettyman

A thesis submitted in partial fulfillment
of the requirements for the degree

of

MASTER OF SCIENCE

in

Civil and Environmental Engineering

Approved:

_____   _____

Michael C. Johnson   Joseph A. Caliendo
Major Professor   Committee Member

_____   _____

Steven L. Barfuss   Mark R. McLellan
Committee Member   Vice President for Research and
                                            Dean of the School of Graduate Studies

UTAH STATE UNIVERSITY
Logan, Utah

2014

ABSTRACT

Considerations for Hood Placement and Design Downstream from a Fixed-Cone Valve

by

Barry J. Prettyman, Master of Science

Utah State University, 2014

Major Professor: Dr. Michael C. Johnson
Department: Civil and Environmental Engineering

Fixed-cone valves, also known as Howell-Bunger valves, are devices often used

to safely reduce flow energy at dams with medium to high heads. The valve directs the

outflow into a conical hollow jet, which requires a large area for energy dissipation. The

flow is controlled by an adjustable sleeve, also known as the gate which surrounds the

valve and requires minimal power for operation even for large valves. Depending on the

installation, the conical jet may need to be controlled by installing a fixed stationary hood

or other structure to contain and direct the conical jet. While the hood reduces the spray,

the use of the hood causes the formation of a concentrated hollow jet having a high

velocity. To eliminate the hollow jet and dissipate much of the associated energy, the

hood can have interior baffles. If the hood is not precisely placed relative to the valve, a

phenomenon, known as backsplash, will occur. Backsplash is when a significant amount

of water exits the upstream end of the hood. Backsplash is a concern for operators

because it can prevent access to the valve during operation and can flood valve vaults. In

low temperatures backsplash will cause ice to form which could also affect the operation

of the valve. This study focuses on the installation requirements and guidelines for

baffled hoods so that backsplash is prevented.

(84 pages)

PUBLIC ABSTRACT

Considerations for Hood Placement and Design Downstream from a Fixed-Cone Valve

Barry J. Prettyman

In many hydroelectric projects there is a need to safely dissipate the energy associated with the elevation of the water surface. When the flow is not passing through the turbines, bypass valves are often used. A valve that is commonly used is the fixed-cone valve. Fixed-cone valves, also known as Howell-Bunger valves, are devices often used to safely reduce flow energy at dams with medium to high heads. The valve directs the outflow into a conical hollow jet, which requires a large area for energy dissipation. The flow is controlled by an adjustable sleeve, also known as the gate which surrounds the valve and requires minimal power for operation even for large valves. Depending on the installation, the conical jet may need to be controlled by installing a fixed stationary hood or other structure to contain and direct the conical jet. While the hood reduces the spray, the use of the hood causes the formation of a concentrated hollow jet having a high velocity. To eliminate the hollow jet and dissipate much of the associated energy, the hood can have interior baffles. If the hood is not precisely placed relative to the valve, a phenomenon, known as backsplash, will occur. Backsplash is when a significant amount of water exits the upstream end of the hood. Backsplash is a concern for operators because it can prevent access to the valve during operation and can flood valve vaults. Because the use of fixed-cone valves and baffled-hoods are becoming more popular, the

need for guidelines to correctly position the hood relative to the valve will benefit both engineers and contractors.

In some hydroelectric sites, submerging the fixed-cone valve is used to control the spray and dissipate energy. Submerging the valve can have can produce violent flow conditions which can cause damage to a structure or heavy erosion. The use of a submerged fixed-cone valve is rarely used, and a submerged valve used with a baffled-hood has never been constructed. The study performed shows that the use of a baffled hood with a fixed-cone valve in submerged conditions performs well. The results may lead the way for more submerged fixed-cone valves in the future.

ACKNOWLEDGMENTS

CONTENTS

LIST OF TABLES

LIST OF FIGURES

NOTATION

cm	=	centimeter
D	=	diameter of the fixed-cone valve
E	=	energy
F	=	force
FCV	=	fixed-cone valve
fps	=	feet per second
g	=	acceleration due to gravity
L	=	distance used to position hood
mm	=	millimeter
P	=	Pressure
P_{ower}	=	power of the flow at specific location
Q	=	discharge rate
V	=	average pipe velocity
V_{exit}	=	average pipe velocity at the hood exit
γ	=	unit weight of water
ρ	=	fluid density

CHAPTER I

INTRODUCTION

When operating hydroelectric power turbines there is a need for turbine bypass valves. The valves are used to bypass turbines when service is required, generating turbines trip off line, or down stream flows must be met. Flow that bypasses a turbine usually has high energy that must be safely dissipated. One method for dissipating this energy is the use of a fixed-cone valve (FCV). FCVs are also known as Howell-Bunger valves and hollow-cone valves. FCVs are used to control flow and dissipate energy under medium to high head conditions. The valve forces the outflow into a diverging conical hollow jet, which produces a large area of energy dissipation through dispersion. The flow can be controlled by a concentric adjustable sleeve, also known as the gate which surrounds the valve. Depending on the installation, the conical jet may need to be controlled. A stationary hood can be placed over the conical jet as shown in Fig. 1.
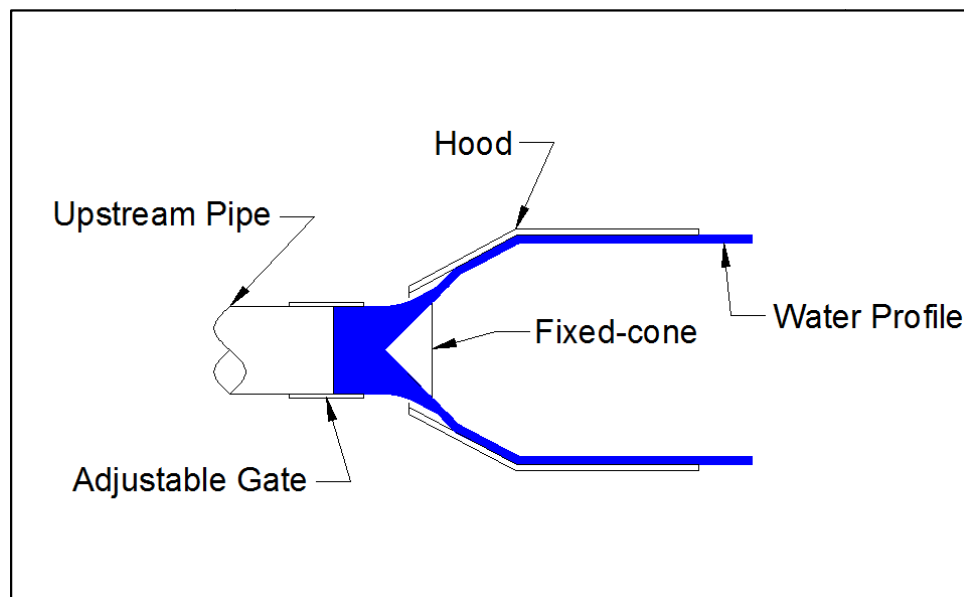
Fig. 1. Fixed-cone valve and hood.

While the hood reduces the spray, the use of the hood causes the formation of a concentrated hollow jet having a high velocity. To eliminate the hollow jet and reduce exit velocities, the hood can include baffles attached to the interior walls. The baffles in the hood dissipate the energy effectively and significantly reduce the area affected by spray (Johnson et al. 2001). Because the performance of the FCV with baffled hoods has been proven to be beneficial, many new installations are being used. With the use of the baffled hood becoming more prominent, this study addresses the backsplash problem that is common with FCVs and baffled hoods and presents considerations and guidelines that effectively eliminate the problem.

One common concern when installing a hood around the FCV is that of backsplash. Backsplash occurs when a significant amount of water exits the upstream end of the hood. For the purposes of this paper, 0.5 percent of the flow exiting the upstream end of the hood would be excessive and would require modifications. This usually occurs when the hood is improperly placed. Backsplash can also occur due to the baffle configuration in the hood (Stephens et al. 2012). Fig. 2 shows severe backsplash occurring with an improperly designed valve and hood combination. Backsplash is a concern because it can prevent access to the valve during operation and valve vaults can be flooded. If low temperatures are present the backsplash will cause ice to form which could affect the operation of the valve (Johnson and Dham 2006).

Fig. 2. Backsplash occurring with a hooded-FCV.

An earlier study was performed to show proper positioning of the hood to prevent backsplash (Kawashima 1984), but the study focused only on one hood and the hood did not contain baffles.

The primary objectives of this thesis were as follows:

1) Determine the placement of a baffled hood around the FCV to improve backsplash performance.

2) Find a modification that can be attached to the FCV to improve backsplash performance.

3) Determine the effects that placing a baffled hood around a FCV have on operations under submerged conditions.

4) Observe the effect that baffle removal has on energy dissipation.

The thesis document will begin by presenting previous literature knowledge on the subject and on operations that are currently in use. The literature review will be followed by the setup of the tests and the actual procedures that were used to improve

backsplash performance. Then the paper discusses models that were tested as a result of

the findings. Finally the results are discussed and presented to demonstrate the benefits of

this study.

CHAPTER II

LITERATURE REVIEW

Crow and Washbourn conducted a study to evaluate the trajectory of the hollow jet of a FCV in free discharge situations (Crow and Washbourn 1985). This was done so a catchment could be sized based on the size, shape, and trajectory of the jet. The valve used was a 1:14.2 scale model of a valve having a 90-degree cone. The valve discharged into a large tank and water was recirculated using a pump. The maximum head was 10 meters and the maximum flow rate was 0.1 m^3/s. To measure the shape and trajectory of the outer boundary of the jet near the valve, the authors used a point gauge mounted on the valve centerline. The gauge could move in both the x (horizontal) and y (vertical) directions. To measure the trajectory of the entire jet, plumb bobs were hung from scaffolding above the centerline and dropped until the bob intercepted the jet. The authors formed Eq. 1 to show jet efficiency.

$$\eta = 96.8 - 1.28F \tag{1}$$

where η is jet efficiency (actual range/theoretical range), and F is the jet Froude number $F = \sqrt{H/t}$, where H is the total head at the valve and t is the thickness of the jet at the vena contracta. The efficiency demonstrates how the height of the hollow jet in relation the velocity head. An initial jet angle was found and compared to the valve opening (stroke or S) in comparison to the diameter (D) of the fixed cone valve (S/D).

Johnson and Dham conducted a study to find alternative means to dissipate energy exiting FCVs using different types of hoods fitted with deflector rings, baffles, and a backsplash suppression ring (Johnson and Dham 2006). To determine how

effective each design was, energy was measured upstream from the valve and

downstream from the hood and the power dissipation was measured using Eq. 2.

$$P_i = \gamma Q (H_i - H_e)$$ (2)

where P_i is the power dissipation, γ is the unit weight of water, Q is the volumetric flow

rate of water, H_i is the total energy at the inlet of the valve, and H_e is the total energy at

the exit of the hood. To determine the energy upstream from the valve, the pressure and

velocity were measured using a pressure gage and an orifice plate, respectively. To find

the energy downstream from the hood, the pressure was assumed to be atmospheric or

zero. The velocity was found by placing a load cell between two plates just downstream

from the end of the hood. The exiting water impacted the plate which allowed a force to

be calculated using the momentum equation and the average velocity was found using

Eq. 3.

$$V_{exit} = \frac{F}{\rho Q}$$ (3)

where V_{exit} is the average velocity of the exiting jet, F is the force of the jet on the load

cell, ρ is the density of water, and Q is the volumetric flow rate. The valve that was used

in the study was a 200 mm FCV. The authors used deflectors and baffles and showed that

baffles were able to dissipate energy more effectively that the deflectors. Fourteen

different configurations of hoods were tested. The authors noted that the hoods emitted

varying amounts of backsplash depending on the configuration. The hood that was

ultimately used had an inside diameter of 590 mm and was 860 mm in length. The final

hood had a backsplash suppression ring with three rows of staggered baffles. This

configuration had no backsplash and had a power dissipation of 92 percent. Of particular note was that the valve's stroke was limited to approximately 55 percent of full open.

The Rodney Hunt Company provided valves to replace two 78-inch butterfly valves used for emergency draining of the Salt Springs Dam (Johnson et al. 2005). As part of the hydroelectric relicensing of the project, minimum instream flows, pulse flows, recreation flows, and flow ramping rates were necessary. The existing 78-inch butterfly valves were not suitable for flow regulation. Instead, two FCVs would replace one of the valves. A 78-inch FCV and a 24-inch FCV, both with stationary hoods, were chosen. The environment surrounding the valves required that the hoods be smaller than the normal design. The normal design of the hood is to have an inside diameter of 2.5 times the diameter of the FCV but, because of the agreements signed, the hood diameter was designed to be 2 times the nominal diameter of the FCV. The testing was performed at the Utah Water Research Laboratory (UWRL) in Logan, Utah in July of 2013. Specific flow rates and pressures were chosen to effectively model the prototype conditions. At each of the flow rates the amount of backsplash was observed. This proved to be difficult because backsplash could not be eliminated and it was determined that the hood diameter would have to be increased. It was found that a hood, with a diamter of 2.2 times the nominal diameter of the FCV, performed well over the expected flow ranges with little backsplash. At commissioning, testing was completed to verify results. Commissioning showed that the valve would operate at the required flow rates and could even operate at higher flow rates with little or no backsplash.

Kawashima studied how the placement of a hood around a FCV affected backsplash performance (Kawashima 1984). The hood used in the study was a combination of cone and cylinder also known as a conventional hood. The conical end being upstream expanding conically to the cylindrical end of the hood. The authors found that the angle of the conical section of the hood and the relative length (L) from valve to hood were the key factors in backsplash performance. The relative length was measured from the projected contact point of the cone to the point of transition from cone to cylinder on the hood as shown in Fig. 3. First the author found a relation between stroke and backsplash. At different hood positions the valve was stroked and the backsplash was measured.
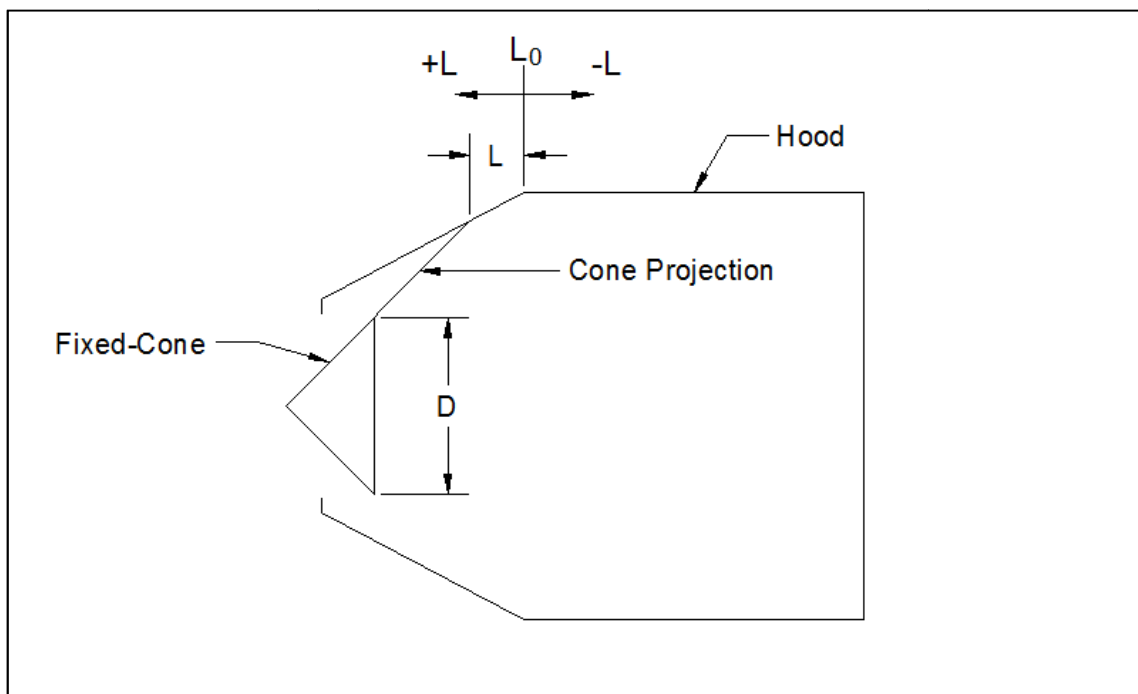
Fig. 3. Relative length developed by Kawashima.

To provide dimensionless units, the author compared the stroke (S) and relative length (L) to the diameter of the valve (D). The author found that at nearly any position of hood, when the stroke was large (S/D > 0.4), there was minimal backsplash. A range was found when the backsplash would increase as the stroke increased (0 < S/D < 0.2) then decreased as the stroke increased (S/D > 0.2). The author then focused on the relationship between backsplash, position of the hood, and angle of the water jet. It was found that positioning the hood too close to the valve (L < 0) caused the water to impact in the cylindrical section of the hood and created a large contact angle (β). This large angle causes the water to exit the upstream end of the hood. As the hood was moved away from the valve the jet impacted the conical section of the hood angle of contact was reduced and the performance improved. Kawashima recommended that the hood be positioned so that L/D was approximately 0.1.

Mefford studied the velocity distribution downstream from the FCV using air as the test fluid (Mefford 1982). Assuming that the velocities were symmetrical the velocities were measured from the centerline of the valve to the edge. The velocities were recorded and streamlines were developed. The streamlines showed that mixing occurs between the jet and the nearby fluid. The fluid directly downstream of the FCV flows toward the valve which creates a stagnation point at the centerline of the valve. Further downstream it was found that the jet reforms with the maximum velocity at the centerline showing that, instead of a submerged conical jet, the flow collapsed on itself and formed a small circular jet with high velocities at the centerline of the valve.

The author was made aware of the Lenihan Dam project wherein FCVs and baffled hoods were placed in operation. The configuration used was a cylindrical baffled hood with a backsplash suppression ring. An email was sent to the Santa Clara Valley Water District to verify how the FCVs were performing at the Lenihan Dam Outlets. The email was sent to obtain information about the operation, performance, and maintenance of the FCVs and the baffled-hoods. The responder was the water resource supervisor Jerry Sparkman. He indicated that the FCVs are fairly new so there is no data on the long-term performance. There are two parallel FCVs installed, a 36-inch diameter and a 16-inch diameter. The area has been in a drought which limits the use of the larger valve. The smaller FCV has been under almost constant operation since its installation and has had no operation problems. The hood in use with the 16-inch FCV has been performing well with the exception of a small amount of backsplash at certain low flow rates. Maintenance of the valves consists of a yearly inspection which entails a visual inspection of the baffles, lubrication of all moving parts, and stroking the FCVs fully opened and closed.

Stephens, Johnson, and Sharp studied the effects that baffles have on energy dissipation and backsplash when used with hoods that have joined conical and cylindrical sections, also known as conventional hoods (Stephens et al. 2012). The authors used computational fluid dynamics (CFD) and some physical models for their investigation. A three-dimensional (3D) model was used to test a 60-inch FCV having an included cone angle of 90 degrees. The diameter of the hood was 150 inches at an included angle of 56 degrees. The baffles were designed by varying the following: the spacing between each

row of baffles, the initial spacing of the first row of baffles from the cone to cylinder

intersection, the height of each baffle, the total number of baffles, and the number of rows

for the total number of baffles. To measure the amount of energy dissipated for each

configuration the energy was measured upstream from the FCV and downstream of the

baffled hood. Forty CFD models were tested and the models were used to help the

authors select a physical model for testing. The CFD models showed that tall baffles with

minimal rows provided the best energy dissipation. After the CFD modeling was

completed, scaled physical models were constructed using Froude similarity. Four

configurations were chosen and compared to the CFD model. The results showed that the

CFD model was fairly accurate for calculating power dissipation, however; the CFD

model did not show the presence of backsplash. Many of the physical models showed

substantial amounts of backsplash that was unacceptable and because of this the

configurations were modified. It was found that the number of rows and the height of the

baffles had a significant impact on backsplash performance. As a result of this study a

number of configurations were found that had no backsplash and effectively dissipated

the energy.

The studies mentioned primarily dealt with one hood and the problems associated

with backsplash were corrected accordingly, but there are a number of hoods of varying

design and baffle configurations that could be used in conjunction with a FCV. This

study focuses on preventing backsplash in hoods with different angles and diameters and

how the addition of baffles affects the performance of the hood. Another emphasis of this

study is to ascertain if the cone-valve design makes an impact on the performance of the

valve/hood combination by comparing different valve configurations. The use of FCVs in submerged conditions is rare and the addition of baffled hoods has never been studied previously. This study observes the effects that the addition of the baffled hood has on the submerged operation of a FCV and provides results showing the effectiveness of the submerged hood.

CHAPTER III

EXPERIMENTAL LABORATORY METHODS

Hood Design

Part of this study was to observe the backsplash performance of different hood designs. Three hoods were chosen that reflect typical stationary hood designs, except for the extended length of the cylindrical section needed to accommodate baffles. Fig. 4 shows the three hoods and the associated hood dimensions. The dimension D refers to the largest diameter of the cone prior to transitioning into the seat. The diameter of the FCV used in the study was 6 inches and refers to the diameter of end of the cone and excludes the seat ring and seating surface. All the dimensions shown are measurements of the wetted surface or inside dimensions of the hood. The hoods were constructed of 1/4 inch thick steel and a flange was welded on to the upstream end to be able to restrain and adjust the position the hood relative to the valve. Hoods 1 and 2 had conical sections having an angle of 28 degrees. This is a hood design that has been used with and without baffles and has shown excellent backsplash performance. To verify if a shorter cylindrical section and a smaller diameter affected backsplash performance, Hoods 1 and 2 were compared. Hood 3, with an angle of 25 degrees, has performed well in many installations, but has yet to be used with baffles.
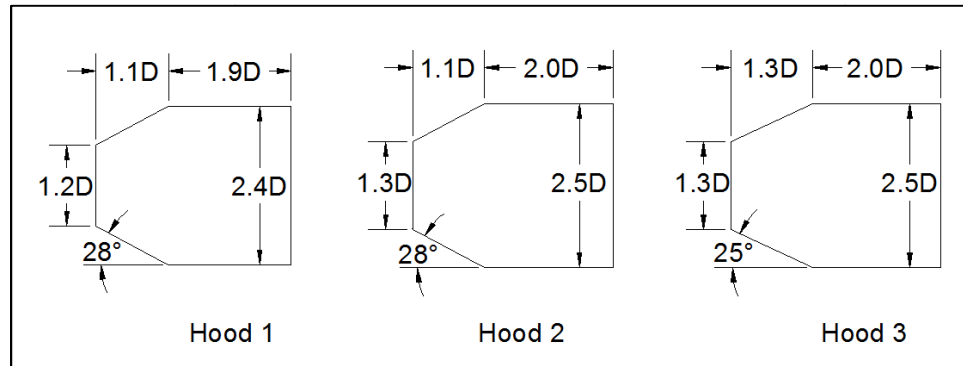
Fig. 4. Three hood dimensions.

Hood Position

Kawashima proved that positioning of the hoods is very important to prevent backsplash (Kawashima 1984). The hood must be centered concentrically on the cone valve and must be positioned precisely. To substantiate the work of Kawashima (1984) and make new discoveries, experiments were performed at the Utah Water Research Lab. The valves were fastened to upstream pipe using four long threaded bolts. This ensured that the valve would be securely fastened and that the valve could be adjusted axially relative to the cone valve. The three hoods were first tested without baffles. Flow rates associated with the tests were measured using a calibrated magnetic flow meter and the upstream pressures were measured approximately two diameters upstream from the FCV using a precision pressure gauge. The testing proceeded as follows: 1) the hood was positioned as deemed acceptable; 2) the valve would be fully stroked at a constant pressure; 3) the pressure would be increased and step 2 would be repeated. If the backsplash amount approached 0.5 percent of the total flow then the steps would be repeated. This was done for each of the hoods shown in Fig. 4.

To verify how the installation of baffles affected the ranges and backsplash performance, each hood had the same baffle configuration installed. Fig. 5 shows the configuration that was installed in every hood. The dimension D is again referring to the largest diameter of the cone. Each hood contained 24 baffles with six baffles in each row. The baffles were placed and staggered so that baffles covered the entire circumference of the cylindrical section of the hood. The baffles were made using pieces of 1/8 inch angle iron and were welded onto the hood. To find the ranges where backsplash performance was acceptable, the steps previously listed were followed.
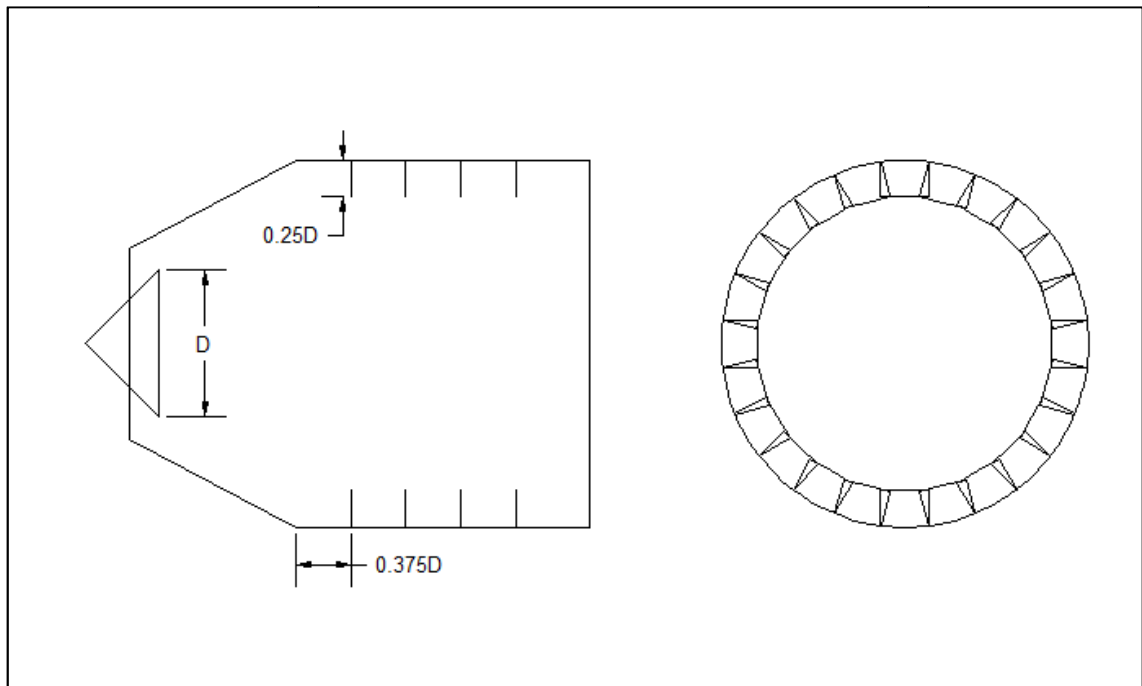
Fig. 5. Configuration with rectangular baffles.

To verify where the conical jet of water was impacting the hoods, the hoods were removed and the outside surface of the hollow conical jet was measured. The following steps were taken when the jet was being measured: 1) the valve was set to a certain opening in percentage; 2) the pressure upstream of the valve was set to pressures of 1, 5, 10, 20, and 30 psi; 3) the horizontal distance to the outer surface of the jet was measured at heights of 5.31, 7.31, and 9.31 inches, using the end of the cone and the axial centerline of the cone as the reference point. Fig. 6 shows the conical jet with the hood removed.

Fig. 6. Photo of conical jet of water.

Cone Valve Design

There are many types of cone valve designs that are used in conjunction with stationary hoods. To verify if certain designs performed better than others, five cone valve configurations were machined. Fig. 7 is a cone-valve design that is common. Fig. 8 shows a close-up view of the seating surface for each valve seat configuration. The cone valve was machined to be able to fasten additional pieces onto the downstream end of the cone facilitating easy alterations. The end plate and spacers were machined on a lathe and holes were drilled in the back so screws could be used to fasten the additions to the downstream end of the cone.

Configuration #1 is representative of a typical FCV with a metal seating surface. Configuration #2 adds an endplate that is slightly larger. Configuration #3 is a combination of the endplate and a spacer. Configuration #4 was done to in an attempt to be more economical by machining an endplate that was larger than the cone but smaller than the endplate in Configuration #2. Configuration #5 is a combination of the smaller endplate with a spacer. Each configuration was installed in the hoods and each was tested to show how it affected backsplash performance. Each cone valve configuration was tested at the pressures and openings that were used when the FCV/hood combinations were tested.
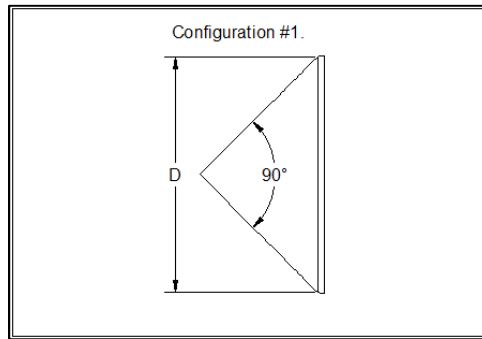
Fig. 7. Typical cone-valve design.
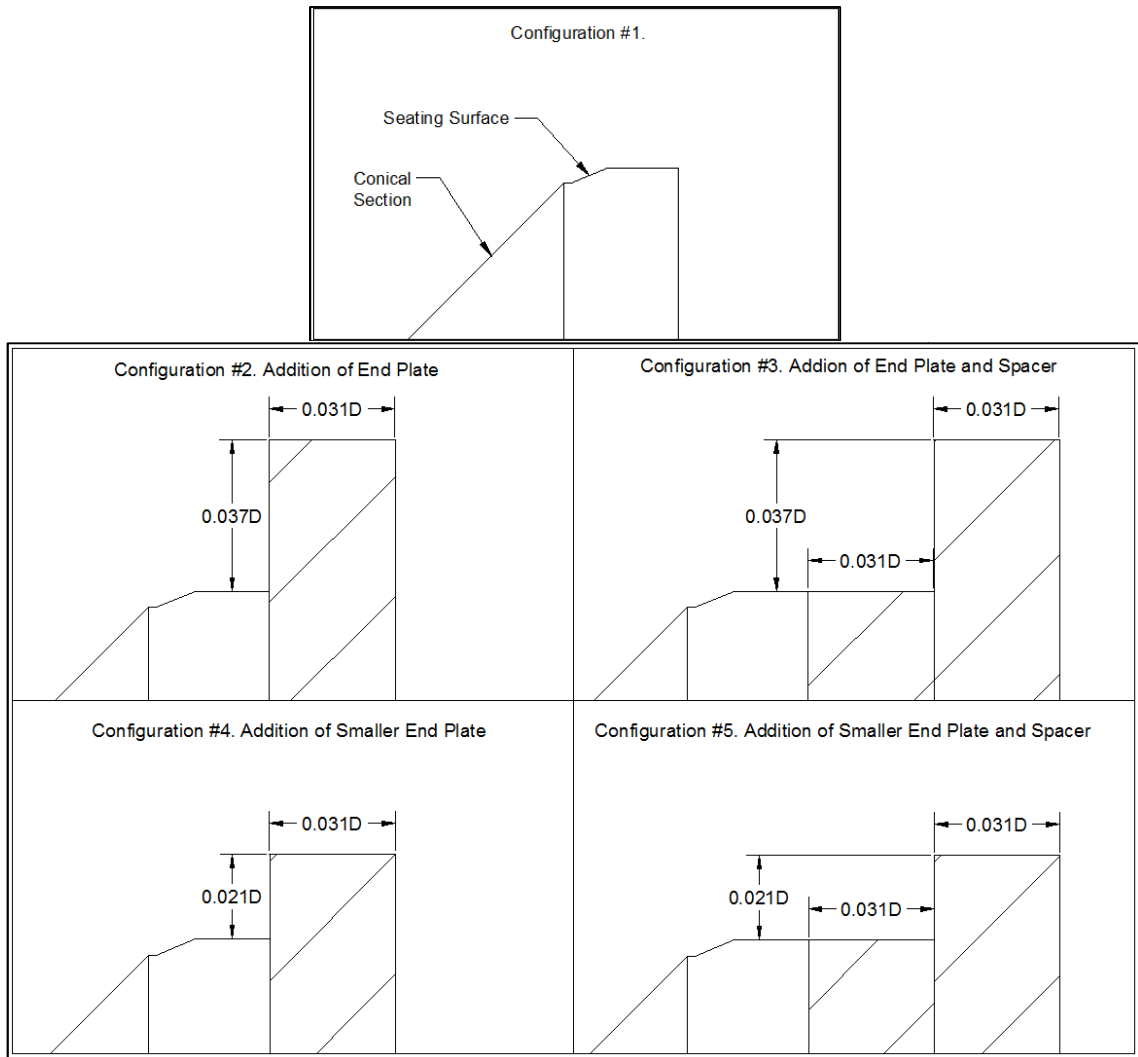
Fig. 8. Cone design configurations.

Baffled Hood under Submerged Conditions

Under most conditions the FCV is discharging into atmospheric pressure and the remaining energy is dissipated in a stilling basin or a discharge channel. The basin or channel is designed to capture the jet and safely dissipate the excess energy. In some cases, submerging the valve can prevent some problems such as a high degree of spray or icing in cold weather conditions (Mefford 1982). Submergence also has negative effects. The potential for cavitation is greater and higher vibrations may occur. The flow pattern is very complex and has the possibility of forming large eddies which can cause problems with sedimentation and erosion. A study was completed which observed the flow pattern of a FCV operating under submerged conditions which showed that, instead of a submerged conical jet, the flow collapses and forms a concentrated submerged jet (Mefford 1982). There is little to no research which investigates the effects that a baffled hood has on the flow pattern when a FCV is submerged.

To understand what effects submerging a FCV with a stationary hood has on velocities exiting the hood, tests were done in the UWRL. Hood 1 was placed in a large box that had adjustable gates that could be closed, allowing for the hood to be completely submerged, or opened, providing free discharge conditions. A 12-inch calibrated magnetic flow meter was used to measure the discharge and a precision pressure gauge was used to measure the pressure approximately 2D upstream from the valve. A pitot-tube and a calibrated pressure transducer were used to measure the velocity profile of the discharge. The pitot-tube measured the total head ($P/\gamma + V^2/2g$) and the piezometric head (P/γ). The calibrated transducer measured the difference of the piezometric head and

total head and an output was given in feet, which represented the velocity head ($V^2/2g$).

Then the velocity was found using the following equation:

$$V = \sqrt{\left(Output - \frac{p}{\gamma}\right)2g}$$

(5)

where V is velocity in, g is the gravitational constant, p is the pressure, and γ is the specific weight of water. The pitot-tube was attached to a 1/8 inch metal strip that was adjustable so the pitot-tube could measure velocities along the axial centerline of the valve as shown in Fig. 9. The hood was tested in free discharge conditions as well as submerged conditions. For both conditions the hood was tested with and without baffles installed. Fig. 5 shows the configuration that was used when baffles were present. The following steps were used to perform the test in free discharge conditions: 1) the valve was set to a specific opening in percent opening; 2) the discharge and upstream pressure were recorded; 3) the pitot-tube measured velocities across the axial centerline; 4) the valve opening was changed and steps 1 through 4 were repeated at openings of 25, 50, 75, 100 percent. The steps for testing the submerged conditions were the same except for the addition of measuring the depth of submergence. This was measured by a calibrated pressure transducer that measured the pressure at the centerline of the valve which was converted to a depth. The submerged depth was approximately 4.4D for all of the tests performed.

Fig. 9. Photo showing velocity measurements at free discharge.

Energy Dissipation

Energy dissipation is one of the most important functions of a baffled hood. Tests were performed to determine the amount of energy dissipated for each row of baffles used. The test was done at the UWRL and because the discharge resulted in a large amount of spray, the hood was encased in a large wooden box.

Hood 1 was used and initially the hood contained 24 baffles with 4 rows of 6 baffles per row. The configuration of the baffles is shown in Fig. 5. To measure the amount of power dissipation associated with the hood, the power upstream and downstream of the hood needed to be calculated. The power at the upstream and downstream positions were found using the following equation:

$$P_{ower} = \gamma Q E \tag{5}$$

where γ is the specific weight of water, Q is the volumetric flow rate, and E is the flow energy at the specific location. The upstream energy, E, was calculated using a pressure

gage approximately two diameters upstream from the valve and the velocity was

calculated using the pipe area and the flow rate and Q was measured using a calibrated

magnetic flow meter. Calculating the flow energy at the downstream location was a little

more difficult because the hood was discharging into atmospheric pressure. To calculate

the power at the downstream end of the hood, first the average velocity was calculated

using Eq. 7 (momentum) and Eq. 8 was used to calculate the associated energy, E.

$$V_{exit} = \frac{F}{\rho Q} \tag{6}$$

$$E = \frac{V_{exit}^2}{2g} \tag{7}$$

where F is force, ρ is the density of water, Q is the volumetric flow rate, and g is the

gravitational constant. F was measured using a load cell that was mounted behind the

plate that was perpendicular to flow 6 inches away from the downstream end of the hood

as shown in Fig. 10. Q was measured using a calibrated magnetic flow meter.

The power dissipation associated with the baffled hood was initially measured

with 24 baffles with 4 rows of 6 baffles per row. The power dissipation was measured at

valve openings of 25, 50, 75, and 100 percent, then a row of 6 baffles would be removed,

starting with the row furthest upstream, and the power dissipation would be measured for

the same valve openings. This was repeated until no baffles remained in the hood.
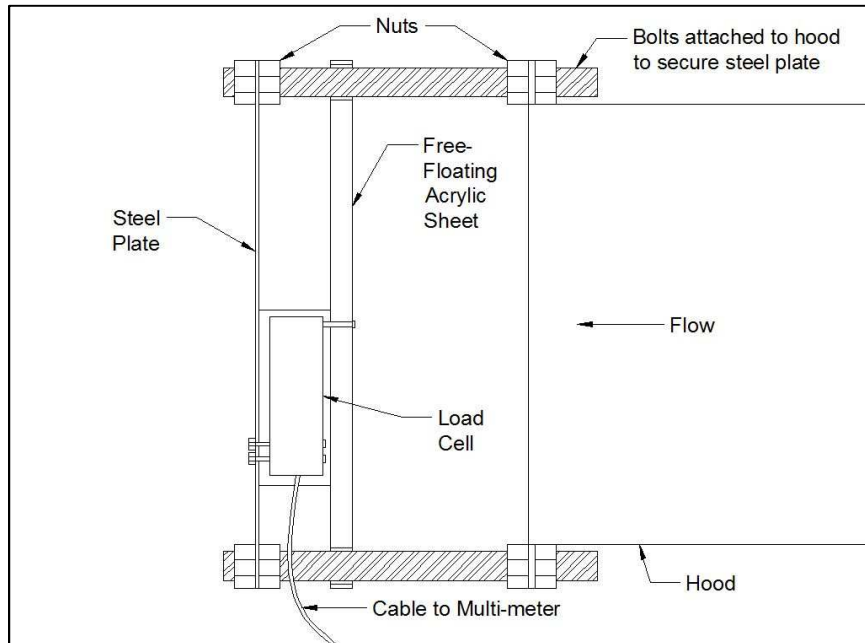
Fig. 10. Acrylic plate and load cell used to measure force.

Fig. 11. Testing setup of downstream power measurement.

CHAPTER IV

RESULTS

Optimal Ranges for Backsplash Performance

Each hood had a range of positions where backsplash was minimal when no baffles were present in the hood. When baffles were installed, the range of good performance was smaller and there was no acceptable range for Hood 3. To help understand where to position the hood, a dimension L was defined. L is an extension of the inside diameter (I.D.) of the hood to the intersection of the projected cone leaving the FCV as shown in Fig. 12. This approach is similar to what FCV manufacturers use when positiong the hood relative to the valve. The projection from the inside diameter was chosen because the thickness of the hood can vary between hoods and the wetted surface was deemed most important. The ranges where the hoods had minimal backsplash are shown in Table 1.
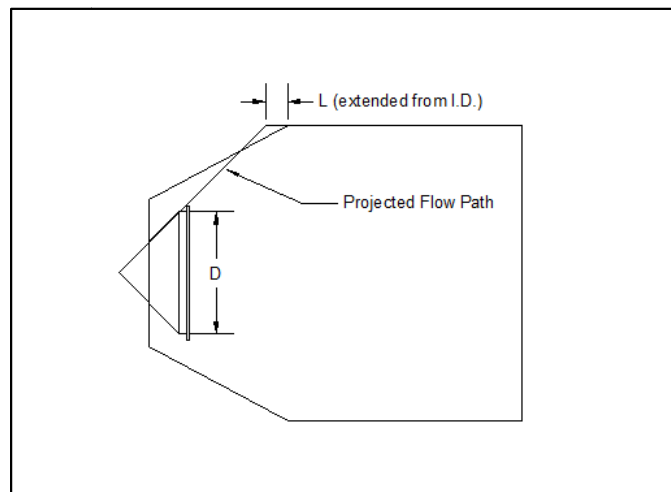
Fig. 12. The dimension L and projected cone.

Table 1. Ranges of hood placement with minimal backsplash.

Baffle Configuration	Hood No.	Range
Without Baffles	1	0.14D - 0.18D
	2	0.16D - 0.20D
	3	0.17D - 0.21D
With Baffles	1	0.15D - 0.17D
	2	0.18D - 0.20D
	3	N/A

The outer surface of the conical jet was measured by removing the hood and measuring the distance to the jet at specific heights, using the end of the cone and the axial centerline as the datum. The measurements were taken at openings of 10, 30, 50, and 100 percent. The pressures were 1, 5, 10, 20, and 30 psi. At the opening of 100 percent the maximum upstream pressure was 5 psi. At 50 percent open the max upstream pressure was 20 psi, and the max for 30 and 10 percent open was 30 psi. The angle of the jet near the valve was measured at each opening. Fig. 13 shows the angle associated with the ratio of valve opening, or stroke (S), to the cone diameter (D). As the valve was opened, the angle became shallower. The measured angle of the jet found during this study agrees with the data collected by Crow and Washbourn (Crow and Washbourn 1985). The impact points for each of the hoods at the varying pressures are shown in Fig. 14 through Fig. 16. These were found by imposing the hood over the cone and then marking the intersection of the hood with the projected jet trajectory. The figures show that for pressures above 5 psi the impact points changed very little. When the pressure was at 1 psi the impact point moved downstream. For the opening of 100% the impact point did not change as the pressure increased.
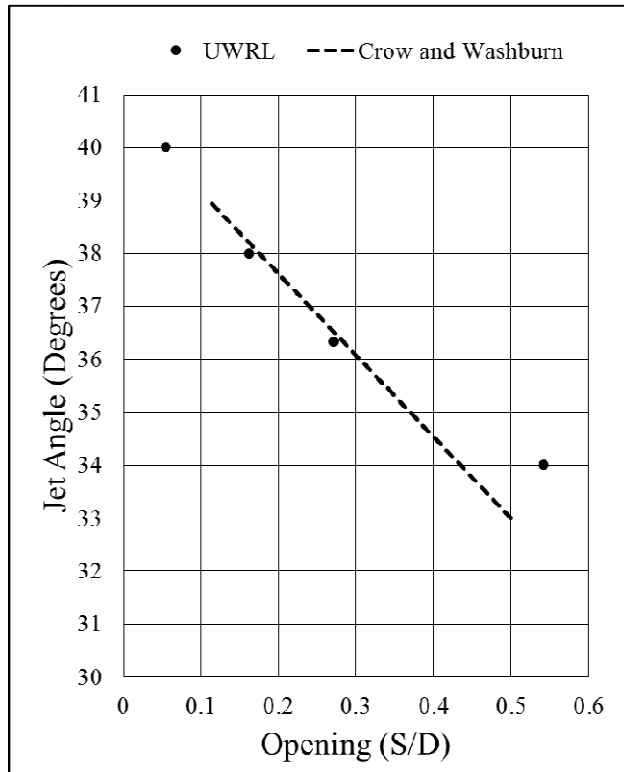
Fig. 13. Initial Jet Angle
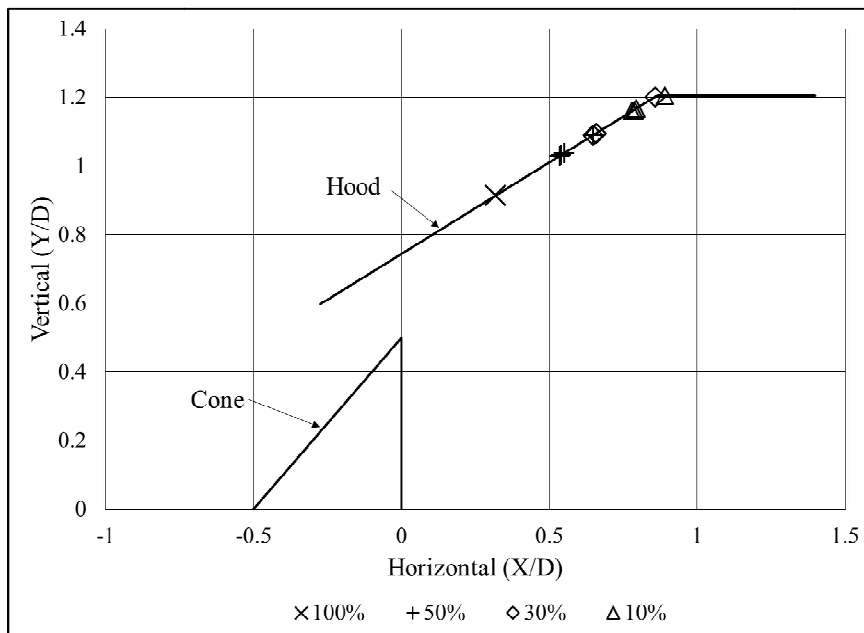
Fig. 14. Outer jet impact locations for Hood 1.
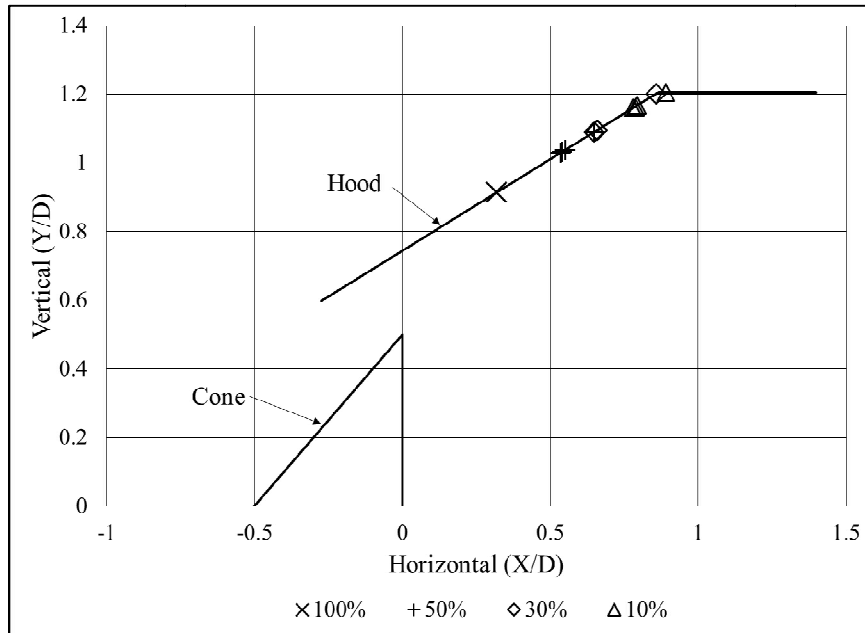
Fig. 15. Outer jet impact locations for Hood 2.
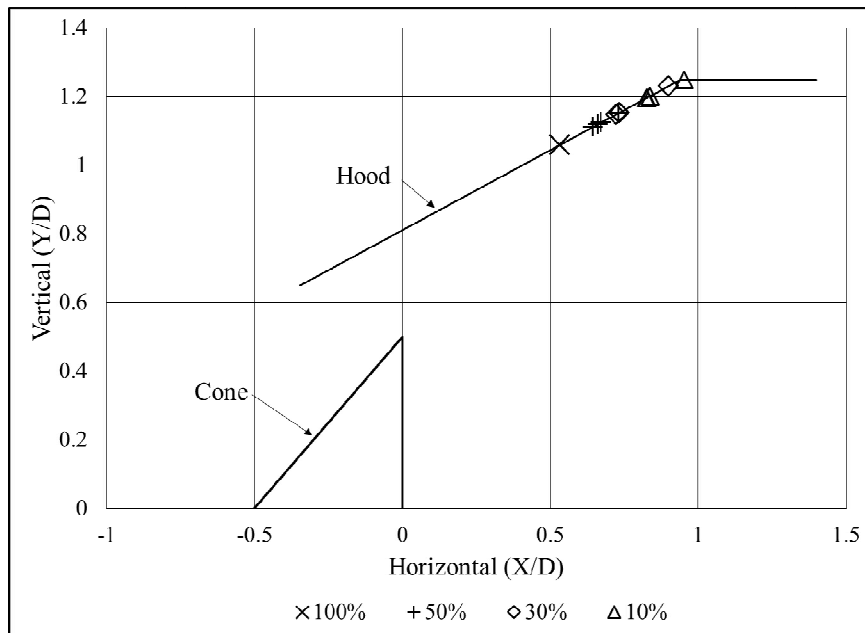
Fig. 16. Outer jet impact locations for Hood 3.

Cone Valve Design

When all the valve designs were tested they were used with each of the three hoods and initially tested within the ranges shown in Table 1. If backsplash was present within the ranges then the hood was adjusted both upstream and downstream in an attempt to stop the backsplash. When there were no baffles in the hoods each of the hoods had ranges that performed well with the varying valve designs. When baffles were introduced, the cone-valve shown in Configuration #3 (as seen in Fig. 8) was the only configuration to have ranges where there was minimal backsplash present. This cone-valve performed well with hoods 1 and 2 (the 28 degree hoods). A range of good performance could not be found for Hood 3. The remaining cone-valve configurations did not have a range where backsplash performance was acceptable in any of the hoods with baffles.

Submerged Baffled Hood

Operating the FCV under a submergence of 4.4D relative to the valve centerline, the velocity profile exiting the hood is shown in Fig. 17 through Fig. 20. At places along the centerline negative velocities were found, indicating that the flow was returning toward the valve. When negative velocities were found they were not plotted. Negative velocities were found when the pitot-tube was downstream of a baffle and when the hood did not have baffles. When the valve and hood without baffles operated under submerged conditions, the majority of the flow was found near the edges of the hood.
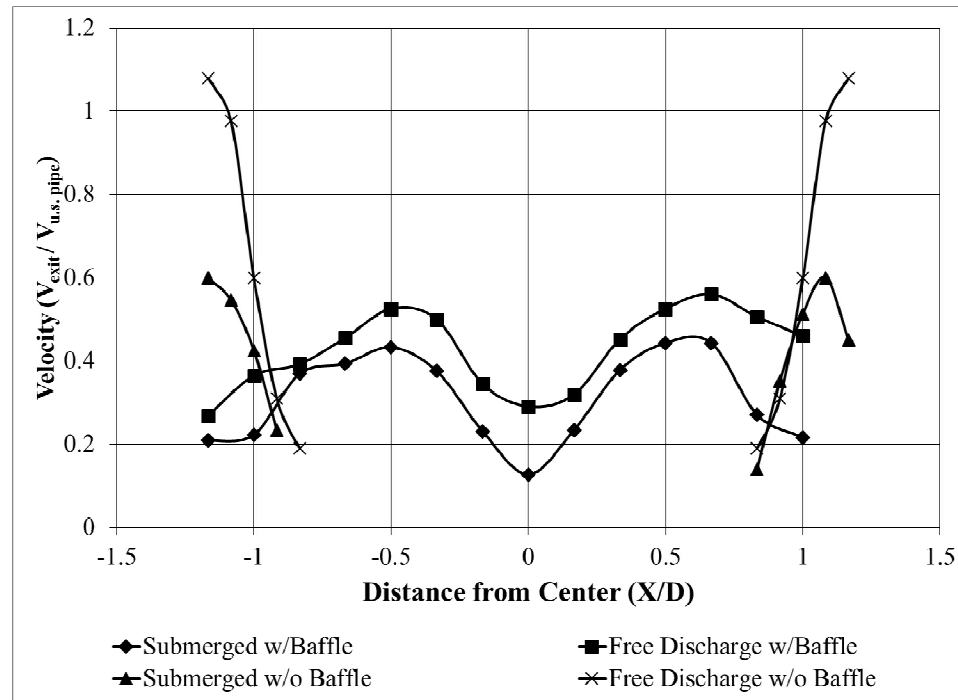
Fig. 17. Velocity profile of 100% open under submerged and free discharge.

In locations other than the edges, the measured velocities were negative values, meaning the flow was collapsing on itself and reversing flow direction. When the valve and hood with no baffles was operated under free discharge conditions, the hood formed a hollow, circular jet and velocities were zero except for the edges. When baffles were attached to the hood, the velocities were the lowest near the center and near the edge of the hood. When compared, the submerged conditions measured lower velocities in all conditions except for the 25 percent opening near the edge of the hood. This shows that submergence dissipates more energy than non-submerged operation.
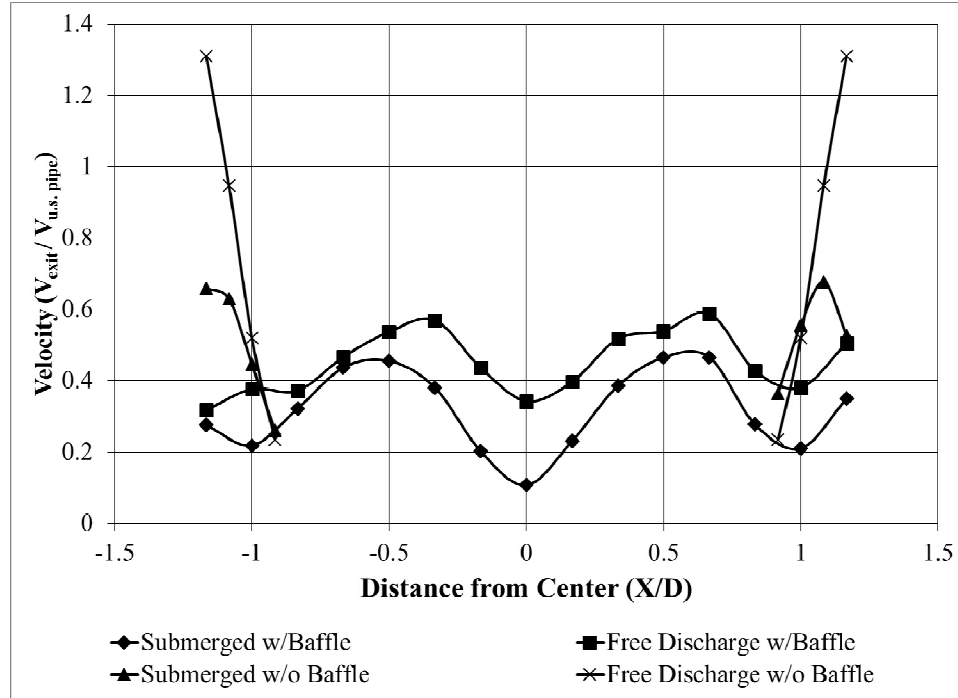
Fig. 18. Velocity profile of 75% open under submerged and free discharge.

Energy Dissipation

Power dissipation was measured for a hood containing 24 baffles, consisting of 4 rows with 6 baffles per row, as shown in Fig. 5. Rows were removed one at a time, starting with the row furthest upstream, to show the associated power dissipation at various openings. Fig. 21 shows the results that removing rows of baffles had on the energy dissipation for different valve openings. As rows were removed, the power dissipation would decrease by a greater amount as shown in Table 2.
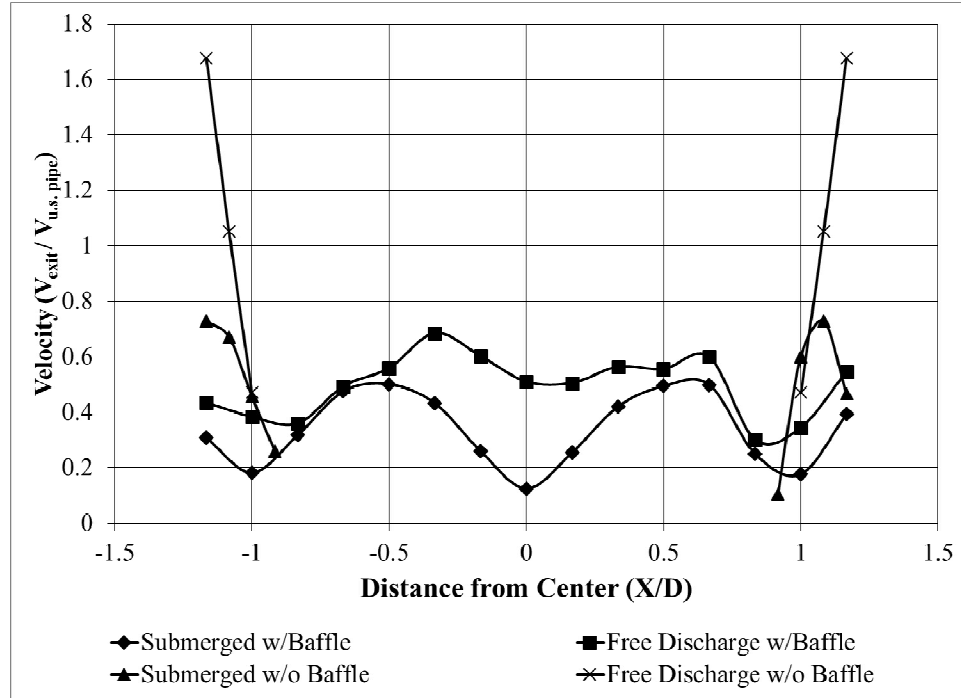
Fig. 19. Velocity profile of 50% open under submerged and free discharge.
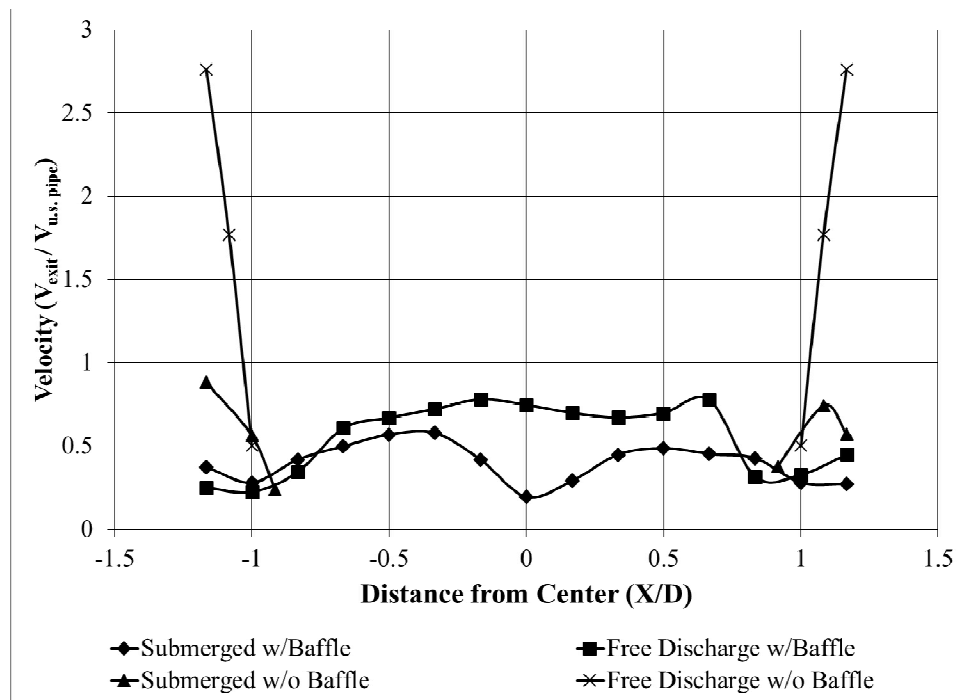
Fig. 20. Velocity profile of 25% open under submerged and free discharge.
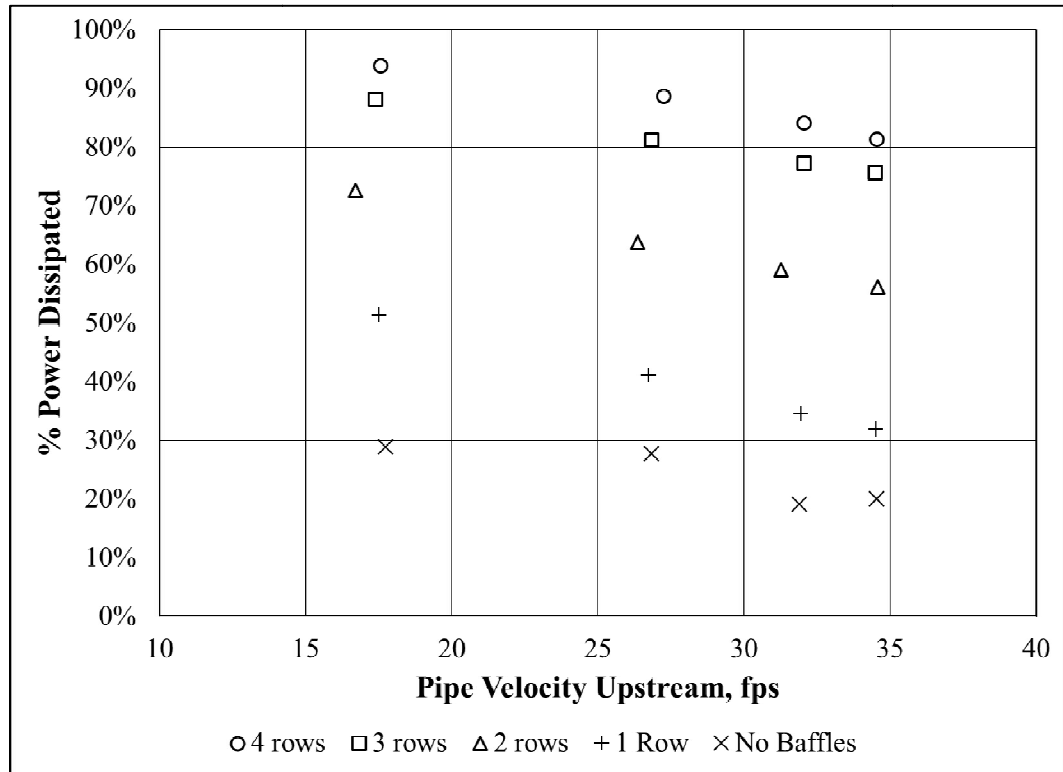
Fig. 21. Power dissipation versus number of baffle rows.

Table 2. Decrease in dissipation for rows of baffles.

No. of Baffle Rows	3	2	1	0
% Decrease in Dissipation	6%	24%	47%	63%

CHAPTER V

DISCUSSION

Hood Placement

Placement of the hood was a very sensitive process. The hood to valve position ranges were fairly small, even when there were no baffles in the hood. The ranges were consistent with Kawashima and hood positions suggested by hood manufacturers. When baffles were introduced in the hood, the placement tolerance became smaller and the position of the hood was extremely sensitive to position and concentricity. Only one baffle configuration (Fig. 5) was studied for the three hoods and the ranges may be specific to that baffle configuration. If another configuration of baffles or different hood design were to be used, it is recommended that additional tests be performed to assure that backsplash is minimal.

The impact points for Hoods 1 and 2 are very similar while the impact points for Hood 3 are further away from the FCV. This is consistent with Kawashima, showing that hood performs better when the jet impacts the conical section of the hood. All hoods had ranges where backsplash was minimal when no baffles were in the hoods. When baffles were added only Hoods 1 and 2 had ranges of minimal backsplash. Hood 3 was moved upstream and downstream from the FCV, in an attempt to prevent backsplash, however, no acceptable range for Hood 3 was found. This shows that when baffles were added, the slight difference of the angle of the conical section of the hood played a significant role in backsplash performance. This helps possible users of FCVs decide which stationary hood would best perform at specific sites. If the site needs to install a baffled hood the 28

degree hood would be preferable, whereas, if there is not a need for baffles in the hood

the 25 degree would perform equally well.

At upstream pressures higher than 5 psi the jet impact points on the hoods did not

change when the pressure was increased. This appears to indicate that the jet geometry is

consistent and the differences are solely related to jet velocity. At pressures lower than 5

psi the impact points began to move downstream. All but one of the points of impact

landed on the conical section of the hood. The point that did not land on the conical

section was at 10 percent open with an upstream pressure of 1 psi. The results show that

the impact locations are mostly independent of pressure (above 5 psi).

Cone-Valve Design

The order of the configurations shown in Fig. 8 are representative of the order in

which they were tested. Configuration #1, which represents a typical, basic metal seated

FCV design was tested and the backsplash was unacceptable despite multiple adjustments

to the hood. Configuration #2 which added an endplate that was slightly larger in

diameter (1.08 D) directly onto the end of the original valve. This design also had poor

backsplash performance. When a spacer was added between the valve and the endplate

(Configuration #3), the backsplash performance improved significantly. The

improvement resulted in essentially eliminating backsplash across the range of flows and

pressures for specific hood locations. After Configuration #3 proved successful, a smaller

endplate was attached without the spacer (Configuration #4) and with the spacer

(Configuration #5). Configurations #1, #2, #4, and #5 had valve openings that performed

well and some that did not perform well. At 100 percent open all of the cone designs

performed well with little to no backsplash. For configurations #1, #4, and #5 backsplash would appear at approximately 70 percent open. As the valve was closed backsplash was present until 30 percent open. Below 30 percent backsplash would be reduced to minimal amounts. Configuration #2 was poor at all openings and it appeared that the jet was impacting the added plate directly because the backsplash was severe.

When Configuration #3 was installed there was an increase in noise, which was a result of an increase in the air demand. The air demand aids in preventing backsplash due to high air velocity at the hood's inlet. When the hood was operating under free discharge conditions, the impact points were measured using the cone configurations #1 and #3. The impact points were essentially the same as shown in Fig. 14 through Fig. 16. These impact points were a measure of the outer diameter of the conical jet of water. The inner diameter of the conical jet was not measured because of the difficulty of measuring the surface. Whether the additional pieces had an impact on the inner jet is unknown. There could be several reasons why the addition of the spacer and plate improve backsplash performance. One possibility is that the water stays attached to the valve, contacts the end plate, which then forces the inner diameter jet to behave differently. The effect on the inner diameter of the jet was not studied, however, it is known that the addition of the spacer and end plate greatly improved the backsplash performance of the valve. The valve was noticeably nosier because the air demand was greater. The most important improvement was the backsplash performance, which resulted in essentially eliminating backsplash.

Submergence

A FCV is not a commonly used energy-dissipator when submerged conditions are present as only two were discovered during the literature review to be operating in submerged conditions. A FCV with a baffled hood operating under submerged conditions could not be found. Previous studies showed that operating a FCV under submerged conditions resulted in the formation of a concentrated submerged jet with high velocities (Mefford 1982). When Logan City operated the FCV at Hydroelectric Project #2, the resulting flows showed that the submerged FCV causes a violent discharge as shown in Fig. 22 through Fig. 23.

The addition of a hood without baffles under submerged conditions showed that the submerged jet attaches to the hood and causes the formation of a concentrated submerged jet with high velocities. The velocities of the submerged conditions were slightly lower than those found at free discharge, however both measured velocities that were high and violent conditions would be expected.

Fig. 22. Operation of Logan Hyrdo #2 FCV.

Fig. 23. Operation of Logan Hyrdo #2 FCV.

When baffles were installed in the hood, the velocities exiting the hood were again lower than those operating at free discharge. The velocity profile suggests that the submerged jet attaches to the hood allowing for the baffles to dissipate energy and reduce velocities.

While there are no known sites that use a FCV with a baffled hood under submerged conditions, the site in Logan, Utah, is implementing a submerged baffled hood. Currently the site, Logan City's Hydroelectric Project #2, has a submerged FCV without a hood that discharges into a chamber having approximately 2D of submergence from the valve centerline. With valve openings of approximately 20 percent and greater, the water in the chamber is evacuated and the valve operates under free discharge. The flow velocities were high enough that the chamber's steel liner was damaged and required repair. A model study was performed at Utah State University that modeled the

site's FCV and the addition of a baffled hood. The study showed excellent results and the baffled hood design will be implemented in 2014.

Energy Dissipation

Tests were performed to show how baffle removal from a hood affected power dissipation when used with a FCV. The rows of baffles were removed one at a time and power dissipation was measured for each row removed. The data for the power dissipation with 24 and zero baffles agree with the previous work done by Stephens et al. (2012) showing that the baffles dissipate a large amount of power. As the rows were removed the decrease in power dissipation increased. Removal of the first row, starting with the row furthest upstream, resulted in a decrease of about six percent after that, the removal of each row resulted in an additional decrease of approximately twenty percent. From this it was calculated that for the first row removed (starting with the furthest row upstream), each baffle removed resulted in a drop of approximately one percent, and after the first row is removed, each baffle removed resulted in a drop of approximately three percent.

CHAPTER VI

CONCLUSIONS

FCVs with hoods have proven to be efficient in energy dissipation and performance when properly installed. If not properly installed, backsplash will be present and could cause problems for operators and the surrounding area. This study provided recommendations that can help clarify how different hoods perform with and without baffles.

The positioning of the hood has a considerable impact on backsplash performance on all the hoods. All of the hoods had ranges of L where backsplash was acceptable when no baffles were installed in the hoods. When the hoods had baffles installed, the angle of the conical section of the hood played a greater role. The 25 degree hood with baffles did not perform as well as either of the 28 degree hoods. The tolerances decreased for both of the 28 degree hoods making the positioning of the hood more important. This will help users who are deciding on what type of hood will be used and if that hood will be baffled. The ranges found for the hoods were for one baffle configuration, so additional studies need to be performed if different baffle configurations are used.

The discovery of the additional spacer and end plate is significant. This configuration was only tested for the baffle configuration done in this study so additional studies may be required for different FCV designs, hood designs and baffle configurations. The effect that the additional spacer and plate (Cone Configuration #3) had on the backsplash performance was unprecedented. The air demand and backsplash performance were drastically changed. If a site was experiencing problems with

performance or backsplash the spacer and the plate could be added to improve performance.

Operating FCVs under submerged conditions is not very common. The valve produces a jet with high velocities that could be unacceptable depending on the site. The addition of the baffled hood resulted in the elimination of the concentrated jet and effectively reduced velocities. With this data, the addition of a baffled hood was recommended for installation at the Hydro #2 in Logan City, Utah. The baffled hood will be installed and is projected to save the city approximately fifty thousand dollars up front by utilizing the hood rather than lining the chamber in stainless steel. The success of this study may result in more submerged FCVs being utilized.

Depending on the site, the energy dissipation may need to be less than that with a hood having a full battery of baffles. This study showed that when baffles are removed the power dissipation decreases about 3 percent with each baffle removed. This information could be useful when designing a stilling basin. This study focused on one baffle configuration so the decreases in power dissipation could be different depending on the number of baffles and the baffle configuration in the hood.

The findings related to the design of the cone-valve are something that requires further research. A better understanding of what occurs near the seating surface of the valve could help understand why the performance improves with the addition of the spacer and end plate. Computational fluid dynamic (CFD) programs could be used to help understand what occurs at such a small scale. Operating a submerged FCV with a baffled hood is also a topic that needs to be researched further as so few are in operation

and the lack of research on the subject. Operating the valve in submerged conditions without aerating the valve results in a higher potential for cavitation which could damage the valve and hood.

As the use of fixed-cone valves with hoods grows, the need for general guidelines to enhance performance increases. This study will help users understand what hood could be used and the placement of the hood so that the valve/hood performs well.

REFERENCES

Crow, D. A., and Washbourn, J. B. (1985). "Investigation into the trajectories of jets issuing from fixed cone valves." *Papers presented at the International Conference on Developments in Valves & Actuators for Fluid Control,* Oxford, England.

Johnson, M. C., and Dham, R. (2006). "Innovative energy-dissipating hood." *J. Hydraulic Engrg.,* 132(8), 759-764.

Johnson, M. C., Dham, R., Sagar, B., and Bergquist, J. (2001, July). "Valves to get out of a fix." *International Water Power & Dam Construction*, pp. 22-25.

Johnson, M. C., Pearman, J. E., and Lubben, R. (2005). "Designing outlet works around a relicense." *Proc., Association of State Dam Safety Officials,* Association of State Dam Safety Officials, Lexington, KY.

Kawashima, M. (1984). "Hydraulic characteristics of hollow cone valve with hood." *Fuji Electric Review,* 22(2), 72-75.

Mefford, B. W. (1982). "Sumberged operation of the fixed-cone valve." PAP 560: Hydraulics Branch Official Copy, Denver, Colorado.

Stephens, D., Johnson, M. C., and Sharp, Z. B. (2012). "Design considerations for fixed cone valve with baffled hood." *J. of Hydraulic Engrg.,* 138(2), 204-209.

APPENDICES

Appendix A: Hood Dimensions and Tolerances
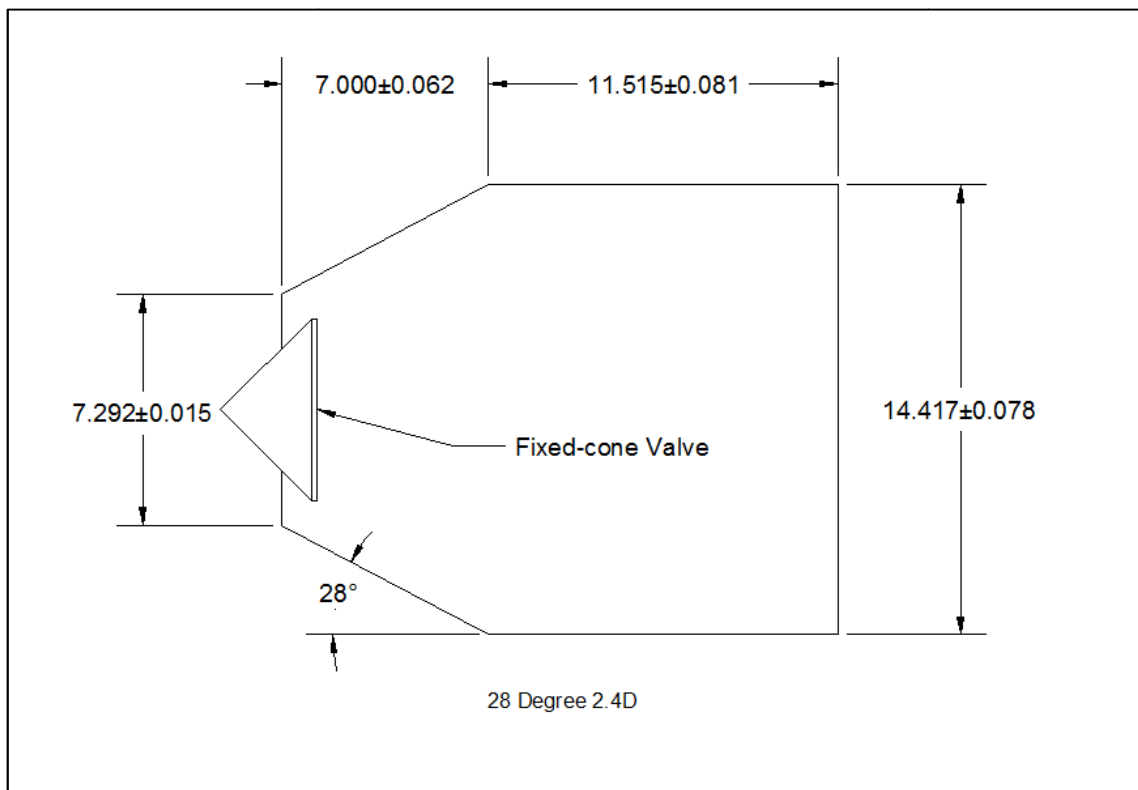
Fig. 24. Dimensions of Hood 1.
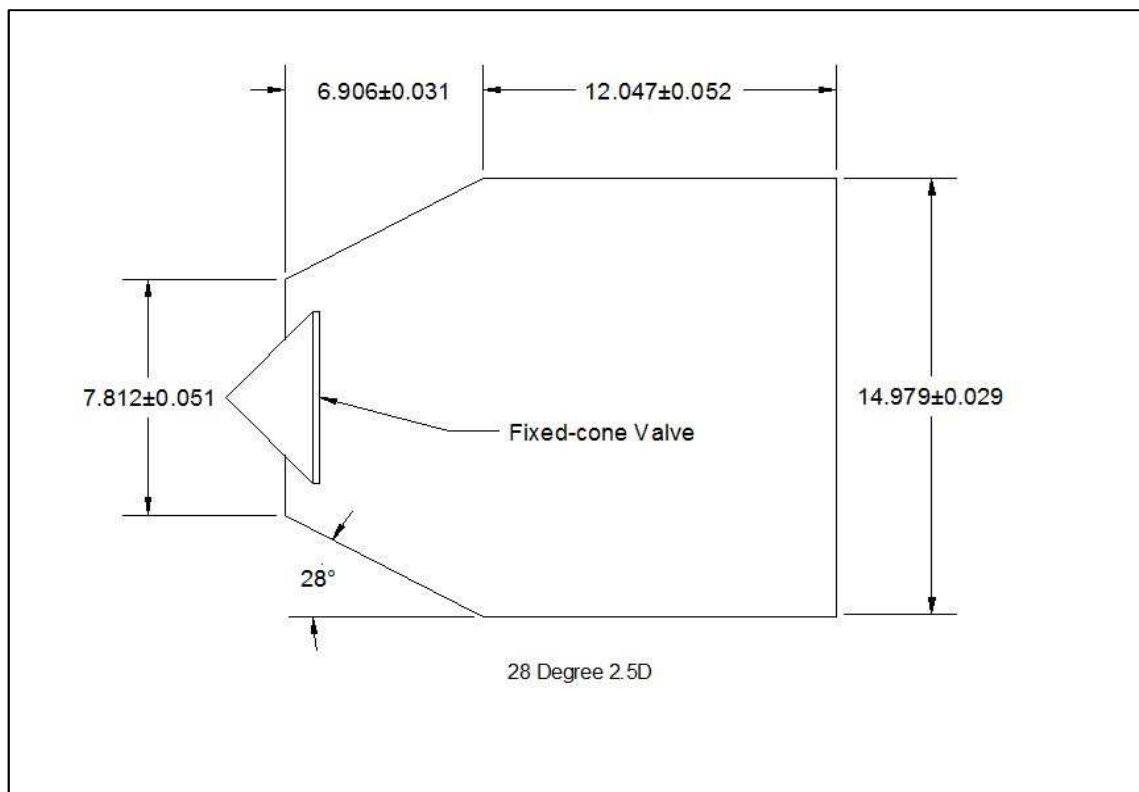
Fig. 25. Dimensions of Hood 2.
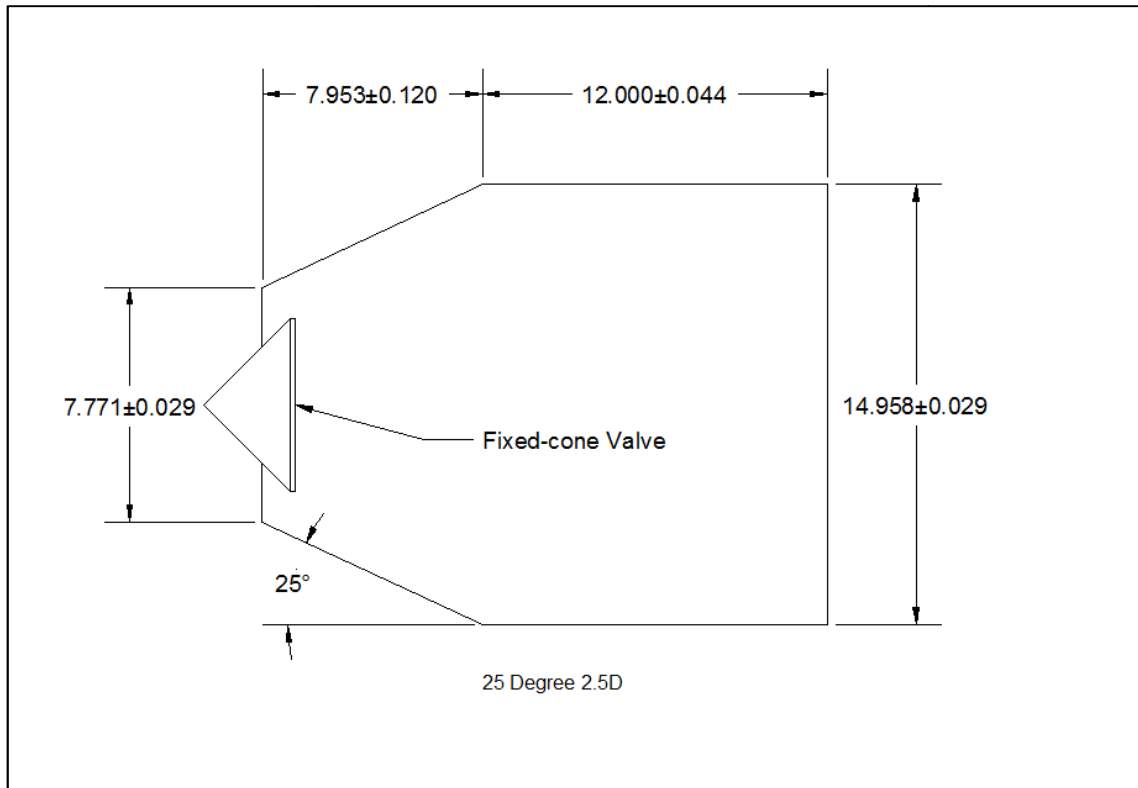
Fig. 26. Dimensions of Hood 3.

Appendix B: Hood Impact Locations

Table 3. Hood 1 impact locations.

Opening (%)	Upstream Pressure (psi)	X (in)	Y (in)
10	*1*	*5.3*	*7.2*
	5	*4.7*	*7*
	10	*4.8*	*7*
	30	*4.7*	*7*
30	*1*	*5.2*	*7.2*
	5	*4*	*6.6*
	10	*4*	*6.6*
	30	*3.9*	*6.5*
50	*1*	*3.9*	*6.5*
	5	*3.2*	*6.2*
	10	*3.3*	*6.2*
	20	*3.2*	*6.2*
100	*1*	*1.9*	*5.5*
	5	*1.9*	*5.5*

Table 4. Hood 2 impact locations

Opening (%)	Upstream Pressure (psi)	X (in)	Y (in)
10	*1*	*5.7*	*7.5*
	5	*4.8*	*7.1*
	10	*4.9*	*7.1*
	30	*4.8*	*7.1*
30	*1*	*5.4*	*7.4*
	5	*4.1*	*6.7*
	10	*4.1*	*6.7*
	30	*4.1*	*6.7*
50	*1*	*4*	*6.6*
	5	*3.4*	*6.3*
	10	*3.5*	*6.3*
	20	*3.4*	*6.3*
100	*1*	*2.1*	*5.6*
	5	*2.1*	*5.6*

Table 5. Hood 3 impact locations

Opening (%)	Upstream Pressure (psi)	X (in)	Y (in)
10	1	5.7	7.5
	5	5	7.2
	10	5	7.2
	30	5	7.2
30	1	5.4	7.4
	5	4.4	6.9
	10	4.4	6.9
	30	4.3	6.9
50	1	4.4	6.9
	5	4	6.7
	10	4	6.8
	20	3.9	6.7
100	1	3.2	6.4
	5	3.2	6.4

Appendix C: Velocity Profile Data

Table 6. Profile data for submerged hood with baffles at 25% open.

Run No.	Flow (gpm)	Pipe Vel. (ft/s)	V. Sub. (ft)	From Center (in)	Inst. Span (in H2O)	Inst. Out (mA)	V. Head (ft)	Velocity (ft/s)
1	1825.50	20.27	2.20	*7.00*	30.00	*7.02*	0.47	5.51
2	1824.75	20.26	2.20	*6.00*	30.00	*7.22*	0.50	5.69
3	1788.00	19.86	2.20	*5.00*	30.00	*11.16*	1.12	8.49
4	1826.25	20.28	2.20	*4.00*	20.00	*16.60*	1.31	9.19
5	1827.75	20.30	2.20	*3.00*	20.00	*18.54*	1.51	9.88
6	1825.50	20.27	2.20	*2.00*	20.00	*16.30*	1.28	9.08
7	1827.00	20.29	2.20	*1.00*	20.00	*9.20*	0.54	5.91
8	1826.25	20.28	2.20	*0.00*	20.00	*6.35*	0.24	3.97
9	1826.25	20.28	2.20	*-1.00*	20.00	*14.68*	1.11	8.46
10	1824.75	20.26	2.20	*-2.00*	30.00	*17.68*	2.14	11.73
11	1823.25	20.25	2.20	*-3.00*	30.00	*17.20*	2.06	11.52
12	1824.00	20.26	2.20	*-4.00*	30.00	*14.15*	1.59	10.11
13	1824.00	20.26	2.20	*-5.00*	30.00	*11.16*	1.12	8.49
14	1825.50	20.27	2.20	*-6.00*	30.00	*7.22*	0.50	5.69
15	1827.00	20.29	2.19	*-7.00*	30.00	*9.75*	0.90	7.61

Table 7. Profile data for submerged hood with baffles at 50% open.

Run No.	Flow (gpm)	Pipe Vel. (ft/s)	V. Sub. (ft)	From Center (in)	Inst. Span (in H2O)	Inst. Out (mA)	V. Head (ft)	Velocity (ft/s)
16	2796.00	31.05	2.20	*7.00*	35.00	*16.68*	2.31	12.20
17	2798.25	31.08	2.20	*6.00*	35.00	*6.60*	0.47	5.52
18	2795.25	31.04	2.20	*5.00*	35.00	*9.16*	0.94	7.78
19	2796.75	31.06	2.20	*4.00*	50.00	*18.35*	3.74	15.51
20	2797.50	31.07	2.20	*3.00*	50.00	*18.10*	3.67	15.38
21	2799.00	31.08	2.20	*2.00*	50.00	*14.18*	2.65	13.07
22	2795.25	31.04	2.20	*1.00*	50.00	*7.75*	0.98	7.93
23	2801.25	31.11	2.20	*0.00*	50.00	*4.91*	0.24	3.91
24	2798.25	31.08	2.20	*-1.00*	50.00	*7.90*	1.02	8.09
25	2798.25	31.08	2.19	*-2.00*	50.00	*14.80*	2.81	13.46
26	2796.75	31.06	2.19	*-3.00*	50.00	*18.46*	3.77	15.57
27	2797.50	31.07	2.18	*-4.00*	50.00	*17.03*	3.39	14.78
28	2799.00	31.08	2.18	*-5.00*	50.00	*9.82*	1.52	9.88
29	2798.25	31.08	2.18	*-6.00*	50.00	*5.93*	0.50	5.69
30	2796.00	31.05	2.18	*-7.00*	50.00	*9.47*	1.42	9.58

Table 8. Profile data for submerged hood with baffles at 75% open.

Run No.	Flow (gpm)	Pipe Vel. (ft/s)	V. Sub. (ft)	From Center (in)	Inst. Span (in H2O)	Inst. Out (mA)	V. Head (ft)	Velocity (ft/s)
31	3391.50	37.66	2.24	*7.00*	50.00	*14.34*	2.69	13.17
32	3395.25	37.71	2.24	*6.00*	50.00	*7.74*	0.97	7.92
33	3393.75	37.69	2.25	*5.00*	50.00	*10.52*	1.70	10.46
34	3394.50	37.70	2.25	*4.00*	65.00	*18.12*	4.78	17.55
35	3392.25	37.67	2.25	*3.00*	65.00	*18.09*	4.77	17.53
36	3393.00	37.68	2.24	*2.00*	65.00	*13.68*	3.28	14.53
37	3393.75	37.69	2.24	*1.00*	65.00	*7.46*	1.17	8.69
38	3395.25	37.71	2.24	*0.00*	65.00	*4.75*	0.25	4.04
39	3392.25	37.67	2.23	*-1.00*	65.00	*6.66*	0.90	7.62
40	3393.00	37.68	2.23	*-2.00*	65.00	*13.45*	3.20	14.35
41	3393.00	37.68	2.22	*-3.00*	65.00	*17.52*	4.58	17.17
42	3393.00	37.68	2.22	*-4.00*	65.00	*16.43*	4.21	16.46
43	3392.25	37.67	2.22	*-5.00*	65.00	*10.74*	2.28	12.12
44	3393.75	37.69	2.22	*-6.00*	65.00	*7.11*	1.05	8.23
45	3393.00	37.68	2.22	*-7.00*	65.00	*8.95*	1.68	10.39

Table 9. Profile data for submerged hood with baffles at 100% open.

Run No.	Flow (gpm)	Pipe Vel. (ft/s)	V. Sub. (ft)	From Center (in)	Inst. Span (in H2O)	Inst. Out (mA)	V. Head (ft)	Velocity (ft/s)
46	3716.25	41.27	2.26	*7.00*	65.00	*11.15*	2.42	12.49
47	3715.50	41.26	2.26	*6.00*	65.00	*7.64*	1.23	8.91
48	3717.75	41.29	2.26	*5.00*	65.00	*9.73*	1.94	11.18
49	3716.25	41.27	2.26	*4.00*	75.00	*17.26*	5.18	18.26
50	3717.00	41.28	2.26	*3.00*	75.00	*17.30*	5.20	18.29
51	3716.25	41.27	2.26	*2.00*	75.00	*13.67*	3.78	15.60
52	3719.25	41.30	2.26	*1.00*	75.00	*7.72*	1.45	9.67
53	3717.00	41.28	2.26	*0.00*	75.00	*5.10*	0.43	5.26
54	3721.50	41.33	2.25	*-1.00*	75.00	*7.61*	1.41	9.53
55	3717.75	41.29	2.24	*-2.00*	75.00	*13.54*	3.73	15.49
56	3722.25	41.34	2.24	*-3.00*	75.00	*16.70*	4.96	17.87
57	3721.50	41.33	2.24	*-4.00*	75.00	*14.53*	4.11	16.28
58	3043.50	33.80	2.23	*-5.00*	75.00	*10.18*	2.41	12.47
59	3719.25	41.30	2.24	*-6.00*	75.00	*7.36*	1.31	9.19
60	3716.25	41.27	2.23	*-7.00*	75.00	*6.95*	1.15	8.61

Table 10. Profile data for submerged hood without baffles at 25% open.

Run	Flow	Pipe Vel.	V. Sub.	From Center	Inst. Span	Inst. Out	V. Head	Velocity
No.	(gpm)	(ft/s)	(ft)	(in)	(in H2O)	(mA)	(ft)	(ft/s)
1	1803.00	20.02	2.20	*7.00*	30.00	*17.08*	2.04	11.47
2	1802.25	20.01	2.23	*6.50*	50.00	*17.20*	3.44	14.88
3	1797.00	19.96	2.24	*5.50*	70.00	*6.44*	0.89	7.57
4	2775.75	30.83	2.23	*5.00*	120.00	*Negative*	-	Negative
4	1785.00	19.82	2.22	*4.00*	50.00	*Negative*	-	Negative
5	1785.75	19.83	2.21	*3.00*	50.00	*Negative*	-	Negative
6	1782.00	19.79	2.21	*2.00*	50.00	*Negative*	-	Negative
7	1780.50	19.77	2.21	*1.00*	50.00	*Negative*	-	Negative
8	1781.25	19.78	2.21	*0.00*	50.00	*Negative*	-	Negative
9	1782.00	19.79	2.21	*-1.00*	50.00	*Negative*	-	Negative
10	1780.50	19.77	2.21	*-2.00*	50.00	*Negative*	-	Negative
11	1780.50	19.77	2.21	*-3.00*	50.00	*Negative*	-	Negative
12	1780.50	19.77	2.21	*-4.00*	50.00	*Negative*	-	Negative
13	1779.75	19.76	2.21	*-5.00*	50.00	*Negative*	-	Negative
14	1800.00	19.99	2.21	*-5.50*	50.00	*5.38*	0.36	4.81
15	1799.25	19.98	2.21	*-6.00*	50.00	*11.52*	1.96	11.23
16	1796.25	19.95	2.23	*-7.00*	70.00	*17.24*	4.83	17.63

Table 11. Profile data for submerged hood without baffles at 50% open.

Run	Flow	Pipe Vel.	V. Sub.	From Center	Inst. Span	Inst. Out	V. Head	Velocity
No.	(gpm)	(ft/s)	(ft)	(in)	(in H2O)	(mA)	(ft)	(ft/s)
17	2832.75	31.46	2.40	*7.00*	70.00	*13.15*	3.34	14.66
18	2833.50	31.47	2.34	*6.50*	120.00	*17.12*	8.20	22.98
19	2833.50	31.47	2.34	*6.00*	120.00	*12.90*	5.56	18.93
20	2832.75	31.46	2.34	*5.50*	120.00	*4.27*	0.17	3.30
21	2775.75	30.83	2.34	*5.00*	120.00	*Negative*	-	Negative
22	1785.00	19.82	2.34	*4.00*	50.00	*Negative*	-	Negative
23	1785.75	19.83	2.34	*3.00*	50.00	*Negative*	-	Negative
24	2773.50	30.80	2.34	*2.00*	120.00	*Negative*	-	Negative
25	2772.75	30.79	2.34	*1.00*	120.00	*Negative*	-	Negative
26	2775.75	30.83	2.34	*0.00*	120.00	*Negative*	-	Negative
27	2775.00	30.82	2.34	*-1.00*	120.00	*Negative*	-	Negative
28	2775.75	30.83	2.34	*-2.00*	120.00	*Negative*	-	Negative
29	1780.50	19.77	2.34	*-3.00*	50.00	*Negative*	-	Negative
30	1780.50	19.77	2.34	*-4.00*	50.00	*Negative*	-	Negative
31	2774.25	30.81	2.34	*-5.00*	120.00	*Negative*	-	Negative
32	2835.00	31.48	2.33	*-5.50*	120.00	*5.67*	1.04	8.20
33	2831.25	31.44	2.33	*-6.00*	120.00	*9.15*	3.22	14.40
34	2831.25	31.44	2.33	*-6.50*	120.00	*15.07*	6.92	21.11
35	2834.25	31.48	2.32	*-7.00*	120.00	*17.05*	8.16	22.92

Table 12. Profile data for submerged hood without baffles at 75% open.

Run	Flow	Pipe Vel.	V. Sub.	From Center	Inst. Span	Inst. Out	V. Head	Velocity
No.	(gpm)	(ft/s)	(ft)	(in)	(in H2O)	(mA)	(ft)	(ft/s)
36	3396.00	37.71	2.28	*7.00*	120.00	*13.82*	6.14	19.88
37	3396.75	37.72	2.23	*6.50*	140.00	*17.85*	10.10	25.50
38	3398.25	37.74	2.22	*6.00*	140.00	*13.37*	6.83	20.98
39	3397.50	37.73	2.22	*5.50*	140.00	*7.99*	2.91	13.69
40	3437.25	38.17	2.22	*5.00*	140.00	*Negative*	-	Negative
41	1785.00	19.82	2.22	*4.00*	50.00	*Negative*	-	Negative
42	1785.75	19.83	2.22	*3.00*	50.00	*Negative*	-	Negative
43	3433.50	38.13	2.22	*2.00*	140.00	*Negative*	-	Negative
44	3435.75	38.15	2.22	*1.00*	140.00	*Negative*	-	Negative
45	3435.00	38.15	2.22	*0.00*	140.00	*Negative*	-	Negative
46	3435.00	38.15	2.22	*-1.00*	140.00	*Negative*	-	Negative
47	3435.75	38.15	2.22	*-2.00*	140.00	*Negative*	-	Negative
48	1780.50	19.77	2.22	*-3.00*	50.00	*Negative*	-	Negative
49	1780.50	19.77	2.22	*-4.00*	50.00	*Negative*	-	Negative
50	3433.50	38.13	2.22	*-5.00*	140.00	*Negative*	-	Negative
51	3397.50	37.73	2.21	*-5.50*	140.00	*6.06*	1.50	9.84
52	3399.00	37.75	2.21	*-6.00*	140.00	*10.04*	4.40	16.84
53	3399.00	37.75	2.22	*-6.50*	140.00	*16.00*	8.75	23.74
54	3397.50	37.73	2.21	*-7.00*	140.00	*17.15*	9.59	24.85

Table 13. Profile data for submerged hood without baffles at 100% open.

Run No.	Flow (gpm)	Pipe Vel. (ft/s)	V. Sub. (ft)	From Center (in)	Inst. Span (in H2O)	Inst. Out (mA)	V. Head (ft)	Velocity (ft/s)
55	3717.00	41.28	2.26	*7.00*	140.00	*11.36*	5.37	18.59
56	3719.25	41.30	2.22	*6.50*	140.00	*17.08*	9.54	24.78
57	3716.25	41.27	2.24	*6.00*	140.00	*13.54*	6.96	21.17
58	3721.50	41.33	2.24	*5.50*	140.00	*8.50*	3.28	14.54
59	3719.25	41.30	2.23	*5.00*	140.00	*4.70*	0.51	5.73
60	1785.00	19.82	2.23	*4.00*	50.00	*Negative*	-	Negative
61	1785.75	19.83	2.23	*3.00*	50.00	*Negative*	-	Negative
62	3765.75	41.82	2.23	*2.00*	140.00	*Negative*	-	Negative
63	3762.75	41.79	2.23	*1.00*	140.00	*Negative*	-	Negative
64	3762.75	41.79	2.23	*0.00*	140.00	*Negative*	-	Negative
65	3763.50	41.79	2.23	*-1.00*	140.00	*Negative*	-	Negative
66	3762.75	41.79	2.23	*-2.00*	140.00	*Negative*	-	Negative
67	1780.50	19.77	2.23	*-3.00*	50.00	*Negative*	-	Negative
68	1780.50	19.77	2.23	*-4.00*	50.00	*Negative*	-	Negative
69	3762.75	41.79	2.23	*-5.00*	140.00	*Negative*	-	Negative
70	3719.25	41.30	2.22	*-5.50*	140.00	*5.97*	1.44	9.62
71	3722.25	41.34	2.22	*-6.00*	140.00	*10.58*	4.80	17.58
72	3724.50	41.36	2.22	*-6.50*	140.00	*14.85*	7.91	22.57
73	3724.50	41.36	2.23	*-7.00*	140.00	*17.10*	9.55	24.80

Table 14. Profile data for free discharge with hood with baffles at 25% open.

Run No.	Flow (gpm)	Pipe Vel. (ft/s)	From Center (in)	Inst. Span (in H2O)	Inst. Out (mA)	V. Head (ft)	Velocity (ft/s)
1	1785.75	19.83	*7.00*	20.00	*15.79*	1.23	8.89
2	1785.00	19.82	*6.00*	20.00	*10.31*	0.66	6.51
3	1785.75	19.83	*5.00*	20.00	*9.90*	0.61	6.29
4	1785.00	19.82	*4.00*	50.00	*18.16*	3.69	15.41
5	1785.75	19.83	*3.00*	50.00	*15.46*	2.98	13.86
6	1782.00	19.79	*2.00*	50.00	*14.54*	2.74	13.30
7	1780.50	19.77	*1.00*	50.00	*15.40*	2.97	13.83
8	1781.25	19.78	*0.00*	50.00	*17.04*	3.40	14.79
9	1782.00	19.79	*-1.00*	50.00	*18.24*	3.71	15.45
10	1780.50	19.77	*-2.00*	50.00	*16.16*	3.17	14.28
11	1780.50	19.77	*-3.00*	50.00	*14.46*	2.72	13.24
12	1780.50	19.77	*-4.00*	50.00	*12.61*	2.24	12.02
13	1779.75	19.76	*-5.00*	50.00	*6.75*	0.72	6.79
14	1780.50	19.77	*-6.00*	50.00	*5.17*	0.30	4.43
15	1780.50	19.77	*-7.00*	50.00	*5.46*	0.38	4.95

Table 15. Profile data for free discharge with hood with baffles at 50% open.

Run No.	Flow (gpm)	Pipe Vel. (ft/s)	From Center (in)	Inst. Span (in H2O)	Inst. Out (mA)	T. Head (ft)	Velocity (ft/s)
16	2774.25	30.81	*7.00*	100.00	*12.48*	4.42	16.87
17	2776.50	30.83	*6.00*	50.00	*10.77*	1.76	10.66
18	2775.00	30.82	*5.00*	50.00	*9.17*	1.35	9.31
19	2774.25	30.81	*4.00*	75.00	*17.58*	5.30	18.48
20	2775.75	30.83	*3.00*	75.00	*15.72*	4.58	17.17
21	2773.50	30.80	*2.00*	75.00	*16.03*	4.70	17.40
22	2772.75	30.79	*1.00*	75.00	*13.68*	3.78	15.60
23	2775.75	30.83	*0.00*	75.00	*13.87*	3.86	15.76
24	2775.00	30.82	*-1.00*	75.00	*17.74*	5.37	18.59
25	2775.75	30.83	*-2.00*	100.00	*17.34*	6.95	21.15
26	2774.25	30.81	*-3.00*	100.00	*12.87*	4.62	17.25
27	2775.00	30.82	*-4.00*	100.00	*10.93*	3.61	15.25
28	2775.00	30.82	*-5.00*	100.00	*7.68*	1.92	11.11
29	2772.75	30.79	*-6.00*	100.00	*8.18*	2.18	11.84
30	2773.50	30.80	*-7.00*	100.00	*9.37*	2.80	13.42

Table 16. Profile data for free discharge with hood with baffles at 75% open.

Run No.	Flow (gpm)	Pipe Vel. (ft/s)	From Center (in)	Inst. Span (in H2O)	Inst. Out (mA)	T. Head (ft)	Velocity (ft/s)
31	3435.00	38.15	*7.00*	100.00	*15.09*	5.78	19.29
32	3433.50	38.13	*6.00*	100.00	*10.29*	3.28	14.53
33	3433.50	38.13	*5.00*	100.00	*11.95*	4.14	16.33
34	3436.50	38.16	*4.00*	100.00	*19.04*	7.83	22.46
35	3437.25	38.17	*3.00*	100.00	*16.62*	6.57	20.57
36	3433.50	38.13	*2.00*	100.00	*15.60*	6.04	19.73
37	3435.75	38.15	*1.00*	100.00	*10.83*	3.56	15.14
38	3435.00	38.15	*0.00*	100.00	*9.10*	2.66	13.08
39	3435.00	38.15	*-1.00*	100.00	*12.26*	4.30	16.64
40	3435.75	38.15	*-2.00*	100.00	*18.07*	7.33	21.72
41	3433.50	38.13	*-3.00*	100.00	*16.50*	6.51	20.48
42	3434.25	38.14	*-4.00*	100.00	*13.44*	4.92	17.79
43	3434.25	38.14	*-5.00*	100.00	*10.00*	3.13	14.19
44	3434.25	38.14	*-6.00*	100.00	*10.15*	3.20	14.36
45	3434.25	38.14	*-7.00*	100.00	*8.36*	2.27	12.09

Table 17. Profile data for free discharge with hood with baffles at 100% open.

Run No.	Flow (gpm)	Pipe Vel. (ft/s)	From Center (in)	Inst. Span (in H2O)	Inst. Out (mA)	T. Head (ft)	Velocity (ft/s)
46	3772.50	41.89	*7.00*	100.00	*15.95*	6.22	20.02
47	3769.50	41.86	*6.00*	100.00	*15.06*	5.76	19.26
48	3768.75	41.85	*5.00*	100.00	*17.36*	6.96	21.17
49	3771.75	41.89	*4.00*	110.00	*18.92*	8.55	23.46
50	3765.00	41.81	*3.00*	110.00	*17.08*	7.49	21.97
51	3765.75	41.82	*2.00*	110.00	*13.68*	5.55	18.90
52	3762.75	41.79	*1.00*	110.00	*8.83*	2.77	13.35
53	3762.75	41.79	*0.00*	110.00	*8.00*	2.29	12.15
54	3763.50	41.79	*-1.00*	110.00	*9.62*	3.22	14.40
55	3762.75	41.79	*-2.00*	110.00	*15.81*	6.77	20.87
56	3762.75	41.79	*-3.00*	110.00	*17.06*	7.48	21.95
57	3763.50	41.79	*-4.00*	110.00	*13.83*	5.63	19.04
58	3762.00	41.78	*-5.00*	110.00	*11.28*	4.17	16.39
59	3762.00	41.78	*-6.00*	110.00	*10.30*	3.61	15.25
60	3763.50	41.79	*-7.00*	110.00	*7.40*	1.95	11.20

Table 18. Profile data for free discharge with hood without baffles at 25% open.

Run No.	Flow (gpm)	Pipe Vel. (ft/s)	From Center (in)	Inst. Span (in H2O)	Inst. Out (mA)	V. Head (ft)	Velocity (ft/s)
1	1746.00	19.39	*7.00*	600.00	*18.25*	44.53	53.55
2	1745.25	19.38	*6.50*	600.00	*9.86*	18.31	34.34
3	1747.50	19.41	*6.00*	600.00	*4.47*	1.47	9.73
4	1745.25	19.38	*5.50*	600.00	*4.00*	-	Inside Jet
5	1785.75	19.83	*5.00*	600.00	*4.00*	-	Inside Jet
6	1782.00	19.79	*2.00*	600.00	*4.00*	-	Inside Jet
7	1780.50	19.77	*1.00*	600.00	*4.00*	-	Inside Jet
8	1781.25	19.78	*0.00*	600.00	*4.00*	-	Inside Jet
9	1782.00	19.79	*-1.00*	600.00	*4.00*	-	Inside Jet
10	1780.50	19.77	*-2.00*	600.00	*4.00*	-	Inside Jet
11	1780.50	19.77	*-3.00*	600.00	*4.00*	-	Inside Jet
12	1780.50	19.77	*-5.00*	600.00	*4.00*	-	Inside Jet
13	1779.75	19.76	*-5.50*	600.00	*4.00*	-	Inside Jet
14	1747.50	19.41	*-6.00*	600.00	*4.47*	1.47	9.73
15	1745.25	19.38	*-6.50*	600.00	*9.86*	18.31	34.34
16	1746.00	19.39	*-7.00*	600.00	*18.25*	44.53	53.55

Table 19. Profile data for free discharge with hood without baffles at 50% open.

Run No.	Flow (gpm)	Pipe Vel. (ft/s)	From Center (in)	Inst. Span (in H2O)	Inst. Out (mA)	T. Head (ft)	Velocity (ft/s)
17	2765.25	30.71	*7.00*	600.00	*17.19*	41.22	51.52
18	2765.25	30.71	*6.50*	600.00	*9.20*	16.25	32.35
19	2764.50	30.70	*6.00*	600.00	*5.04*	3.25	14.47
20	2832.75	31.46	*5.50*	600.00	*4.00*	-	Inside Jet
21	2775.75	30.83	*5.00*	600.00	*4.00*	-	Inside Jet
22	2773.50	30.80	*2.00*	600.00	*4.00*	-	Inside Jet
23	2772.75	30.79	*1.00*	600.00	*4.00*	-	Inside Jet
24	2775.75	30.83	*0.00*	600.00	*4.00*	-	Inside Jet
25	2775.00	30.82	*-1.00*	600.00	*4.00*	-	Inside Jet
26	2775.75	30.83	*-2.00*	600.00	*4.00*	-	Inside Jet
27	2774.25	30.81	*-5.00*	600.00	*4.00*	-	Inside Jet
28	2835.00	31.48	*-5.50*	600.00	*4.00*	-	Inside Jet
29	2764.50	30.70	*-6.00*	600.00	*5.04*	3.25	14.47
30	2765.25	30.71	*-6.50*	600.00	*9.20*	16.25	32.35
31	2765.25	30.71	*-7.00*	600.00	*17.19*	41.22	51.52

Table 20. Profile data for free discharge with hood without baffles at 75% open.

Run No.	Flow (gpm)	Pipe Vel. (ft/s)	From Center (in)	Inst. Span (in H2O)	Inst. Out (mA)	T. Head (ft)	Velocity (ft/s)
32	3384.00	37.58	*7.00*	600.00	*16.04*	37.63	49.22
33	3399.00	37.75	*6.50*	600.00	*10.34*	19.81	35.72
34	3402.00	37.78	*6.00*	600.00	*5.92*	6.00	19.66
35	3398.25	37.74	*5.50*	600.00	*4.39*	1.22	8.86
36	3437.25	38.17	*5.00*	600.00	*4.00*	-	Inside Jet
37	3433.50	38.13	*2.00*	600.00	*4.00*	-	Inside Jet
38	3435.75	38.15	*1.00*	600.00	*4.00*	-	Inside Jet
39	3435.00	38.15	*0.00*	600.00	*4.00*	-	Inside Jet
40	3435.00	38.15	*-1.00*	600.00	*4.00*	-	Inside Jet
41	3435.75	38.15	*-2.00*	600.00	*4.00*	-	Inside Jet
42	3433.50	38.13	*-5.00*	600.00	*4.00*	-	Inside Jet
43	3398.25	37.74	*-5.50*	600.00	*4.39*	1.22	8.86
44	3402.00	37.78	*-6.00*	600.00	*5.92*	6.00	19.66
45	3399.00	37.75	*-6.50*	600.00	*10.34*	19.81	35.72
46	3384.00	37.58	*-7.00*	600.00	*16.04*	37.63	49.22

Table 21. Profile data for free discharge with hood without baffles at 100% open.

Run No.	Flow (gpm)	Pipe Vel. (ft/s)	From Center (in)	Inst. Span (in H2O)	Inst. Out (mA)	T. Head (ft)	Velocity (ft/s)
47	3756.00	41.71	*7.00*	600.00	*14.06*	31.44	45.00
48	3753.75	41.69	*6.50*	600.00	*12.23*	25.72	40.70
49	3756.00	41.71	*6.00*	600.00	*7.11*	9.72	25.02
50	3757.50	41.73	*5.50*	600.00	*4.83*	2.59	12.92
51	3756.75	41.72	*5.00*	600.00	*4.31*	0.97	7.90
52	3765.75	41.82	*2.00*	600.00	*4.00*	-	Inside Jet
53	3762.75	41.79	*1.00*	600.00	*4.00*	-	Inside Jet
54	3762.75	41.79	*0.00*	600.00	*4.00*	-	Inside Jet
55	3763.50	41.79	*-1.00*	600.00	*4.00*	-	Inside Jet
56	3762.75	41.79	*-2.00*	600.00	*4.00*	-	Inside Jet
57	3756.75	41.72	*-5.00*	600.00	*4.31*	0.97	7.90
58	3757.50	41.73	*-5.50*	600.00	*4.83*	2.59	12.92
59	3756.00	41.71	*-6.00*	600.00	*7.11*	9.72	25.02
60	3753.75	41.69	*-6.50*	600.00	*12.23*	25.72	40.70
61	3756.00	41.71	*-7.00*	600.00	*14.06*	31.44	45.00

Appendix D: Power Dissipation Data

Table 22. Power dissipation for hood with 4 rows of baffles.

Run No.	Flow (gpm)	Pipe Vel. (ft/s)	P. Gage (psi)	P. Head (ft)	US Energy (ft)	Load Cell (mV)	Force (lb)	DS Vel (ft/s)	Exit Energy (ft)	Power Diss. (%)
1	3110	34.5	*5.50*	12.7	31.2	*7.80*	260	19.3	5.81	81%
2	2887	32.1	*8.80*	20.3	36.3	*7.20*	240	19.2	5.74	84%
3	2455	27.3	*14.8*	34.0	45.6	*5.80*	193	18.2	5.16	89%
4	1582	17.6	*24.8*	57.1	61.9	*3.20*	107	15.6	3.78	94%

Table 23. Power dissipation for hood with 3 rows of baffles.

Run No.	Flow (gpm)	Pipe Vel. (ft/s)	P. Gage (psi)	P. Head (ft)	US Energy (ft)	Load Cell (mV)	Force (lb)	DS Vel (ft/s)	Exit Energy (ft)	Power Diss. (%)
5	3107	34.5	*5.45*	12.6	31.1	*8.90*	297	22.1	7.58	76%
6	2887	32.1	*8.70*	20.1	36.0	*8.60*	287	23.0	8.20	77%
7	2417	26.8	*15.1*	34.8	46.0	*7.40*	247	23.6	8.65	81%
8	1565	17.4	*24.8*	57.2	61.9	*4.40*	147	21.7	7.30	88%

Table 24. Power dissipation for hood with 2 rows of baffles.

Run No.	Flow (gpm)	Pipe Vel. (ft/s)	P. Gage (psi)	P. Head (ft)	US Energy (ft)	Load Cell (mV)	Force (lb)	DS Vel (ft/s)	Exit Energy (ft)	Power Diss. (%)
9	3114	34.6	*5.30*	12.2	30.8	*11.9*	397	29.5	13.5	56%
10	2817	31.3	*9.70*	22.4	37.6	*11.5*	383	31.5	15.4	59%
11	2375	26.4	*15.7*	36.2	47.0	*10.2*	340	33.1	17.0	64%
12	1505	16.7	*25.4*	58.6	62.9	*6.50*	217	33.3	17.2	73%

Table 25. Power dissipation for hood with 1 row of baffles.

Run No.	Flow (gpm)	Pipe Vel. (ft/s)	P. Gage (psi)	P. Head (ft)	US Energy (ft)	Load Cell (mV)	Force (lb)	DS Vel (ft/s)	Exit Energy (ft)	Power Diss. (%)
13	3109	34.5	*5.50*	12.7	31.2	*14.9*	497	37.0	21.2	32%
14	2877	31.9	*8.90*	20.5	36.4	*14.6*	487	39.1	23.8	35%
15	2408	26.7	*15.3*	35.3	46.4	*13.1*	437	42.0	27.3	41%
16	1577	17.5	*24.8*	57.2	62.0	*9.00*	300	44.0	30.1	51%

Table 26. Power dissipation for hood with no baffles.

Run No.	Flow (gpm)	Pipe Vel. (ft/s)	P. Gage (psi)	P. Head (ft)	US Energy (ft)	Load Cell (mV)	Force (lb)	DS Vel (ft/s)	Exit Energy (ft)	Power Diss. (%)
17	3110	34.5	*5.40*	12.5	31.0	*16.1*	537	39.9	24.8	20%
18	2873	31.9	*8.90*	20.5	36.3	*16.2*	540	43.5	29.4	19%
19	2417	26.8	*15.1*	34.8	46.0	*14.5*	483	46.3	33.2	28%
20	1597	17.7	*24.6*	56.8	61.6	*11.0*	367	53.1	43.8	29%